

Cite this: *RSC Sustainability*, 2025, 3, 4598

# Designing marine-derived carrageenan-based biomimetic functional materials *via* a green approach for sustainable development: cellular proliferation and mucosal tissue drug delivery applications

Nistha Thakur and Baljit Singh \*

The present research aims to explore the potential of marine-derived carrageenan (CG) polysaccharides in developing bioactive materials *via* a green approach for sustainable development, thereby promoting the well-being of society and mitigating human health issues. The health issues prevailing among women, especially those related to female reproductive system, pose a significant challenge globally. Hence, the proposed research work is based on the development of functional materials for the pharmaceutical evaluation of an antibiotic therapeutic agent. These network hydrogels were fabricated *via* a copolymeric reaction of PVP and polyacrylamide onto CG. The network hydrogels have unique traits that make them perfect biomaterials for vaginal drug delivery (VDD) and overcome the limitations associated with conventional VDD. The copolymers were characterized by FESEM, EDAX, AFM, FTIR spectroscopy, <sup>13</sup>C-NMR and XRD techniques. The materials were subjected to multiple performance analyses, including biocompatibility, antioxidation, mucoadhesion, anti-inflammation, protein adsorption, antimicrobial activity, simulated vaginal fluid sorption, drug delivery and cell viability of rhabdomyosarcoma cells to evaluate their biomedical applications. The hydrogels expressed 190% ± 7.07% viability for RD cells and promoted their proliferation, which signified their non-toxic nature to mammalian cells. The hydrogels depicted a 52.40% ± 1.14% scavenging ability against DPPH radicals, which outlined their antioxidant properties. The mucoadhesive performance of the material was expressed by the fact that it required a force of 93 ± 6.11 mN for its separation from the mucosal surface. Additionally, diffusion of the antibiotic agent from the drug-infused hydrogel followed a non-Fickian diffusion mechanism, and the release profile was best interpreted by the Hixson–Crowell kinetic model. The cell viability, non-haemolytic and biomedical properties of the hydrogels emphasize the use of these biomaterials as a sustainable platform for intravaginal drug delivery.

Received 6th June 2025  
Accepted 3rd August 2025

DOI: 10.1039/d5su00412h

rsc.li/rscsus

## Sustainability spotlight

Recently, research has predominately centered on designing materials from natural resources to promote sustainable development. These materials find widespread applications in biomedical fields and creation of health-care products. Marine-derived carrageenan gum, a natural polysaccharide, has been explored for developing materials for drug delivery carriers, and its utilization is a safer and eco-friendly approach aligning with increasing demands for sustainable and biocompatible materials. This work aligns with the UN's Sustainable Development Goals 3 and 9, as it is the sustainable renewable product in the form of bioactive hydrogel wound dressing for good health and well-being.

## 1 Introduction

In recent years, research has progressively focused on the innovation and development of advanced materials to improve human health and address various medical challenges.<sup>1</sup> Natural polysaccharides are recognised and extensively explored for

synthesizing functional biomaterials for innovative drug delivery (DD) systems.<sup>2</sup> Vaginal infections prevailing among women remain a significant challenge globally.<sup>3</sup> Despite the availability of diverse vaginal dosage forms for vaginal infections and other associated disorders, the long duration of therapy remains a pharmaco-therapeutic challenge associated with DD to the vaginal area.<sup>4</sup> These limitations have been addressed through the design of hydrogel materials, enabling their use as highly efficient carriers for VDD.<sup>5</sup>

Department of Chemistry, Himachal Pradesh University, Shimla-171005, India.  
E-mail: baljitsinghpu@yahoo.com



The biocompatibility, tissue-like consistency, mucoadhesion and high water retention capacity of hydrogels are some unique traits that make them perfect biomaterials for VDD. The soft and rubbery nature of fully swollen hydrogels allows them to mimic soft biological tissues, making these materials usable for DD during gynaecological treatment. Swollen mucoadhesive gels ensure uniform distribution of drugs with minimal leakage, which retains the medicine in the vaginal region.<sup>6</sup> An intra-vaginal route is applied for the delivery of antimicrobials, anti-virals, labour inducers, prostaglandins, anti-protozoal drugs and steroid drugs.<sup>7</sup> Conventional VDD formulations (including creams, gels, vaginal suppositories and tablets) suffer from multiple limitations (leakage, spreading of drugs over vaginal surfaces, low drug penetration, vaginal and cervical secretions, smooth muscle contractions and low residence time) during their application to the vaginal region.<sup>8</sup> These formulations are easily eluted with the vaginal fluid, which reduces their ability to stay at the adsorption site and led to incomplete delivery of therapeutic agents. Moreover, when these formulations are exposed to an acidic pH environment of the vagina, they lose their structural integrity, cause local irritation and become less viscous, and hence, the drug is released at a faster rate.<sup>9,10</sup> As a result, multiple doses are often needed daily to achieve the desired therapeutic effects, resulting in poor patient compliance and failure of the desired therapeutic effects along with increased overall treatment costs.<sup>11</sup> Hence, advanced VDD formulation is required to ensure proper release and sustained retention for the intended period to get an improved therapeutic outcome.<sup>12</sup> Furthermore, the sustainability and renewability of biopolymers make them desirable alternatives for the conventional polymers and their functionalization enhances their potential applications in healthcare products.<sup>13</sup>

Hassan and coworkers<sup>14</sup> found that the adhesive properties of chitosan–alginate-based polymeric materials have improved the vaginal DD of progesterone. These hydrogels helped in increasing the drug residence time in the vaginal cavity, allowing better drug absorption and higher bioavailability over a prolonged period. Pérez and coworkers<sup>15</sup> observed that the cellulose–chitosan-based formulations provided sustained drug release and remained adhered to the vaginal mucosa. Hassan and coworkers<sup>16</sup> prepared active luliconazole-loaded nanogels for treating *Candida albicans* and observed that the vaginal gels showed high drug encapsulation, enhanced mucosal permeability and better patient comfort. The nanogels also provided good vaginal-mucosal adhesion to aid formulation retention and sustained drug release. Zhang and coworkers<sup>17</sup> prepared stable estradiol-loaded poly(hydroxyethyl methacrylate)-alginate hydrogels to facilitate vaginal wound repair. These hydrogels provided sustained DD, supported cell growth and collagen deposition, thereby restoring vaginal barrier while maintaining the acidic environment and helped in wound healing. Pattanayak and coworkers<sup>18</sup> designed an antimicrobial agent-incorporated cellulose acetate-based membrane to treat skin infections and resolve concerns related to female hygiene products.

Iota carrageenan (CG) is an anionic sulfated galactan derived from red sea weed, composed of alternating 3-linked  $\beta$ -D-galactopyranose-4-sulphate (G4S units) and 4-linked 3,6-anhydro-

$\alpha$ -D-galactopyranose-2-sulphate (DA2S units). In addition to sulfate groups, xylose, glucose, uronic acids, and methyl esters are also present in CG. CG has multitudinous biological activities including anticoagulant, anti-thrombogenicity, anti-inflammatory, antimicrobial and antitumor properties.<sup>19–21</sup> It is widely used in the pharmaceutical industry and has various DD applications.<sup>22,23</sup> CG has a tendency to form complexes with the drug, and hence, can increase drug loading, improve dissolution rate of poorly water-soluble drugs, and provide sustained drug release.<sup>24,25</sup> Agili and coworkers<sup>26</sup> prepared self-crosslinked CG-poly(acrylamide) (AAM)-based hydrogels with antimicrobial and anti-inflammatory activities for wound healing applications. Perotti and coworkers<sup>27</sup> revealed that CG formulations block the cell trafficking of macrophages from vagina, which may help to prevent sexual transmission of HIV. PVP is a biocompatible and hydrophilic polymer used in the biomedical field. PVP can be blended with other polysaccharides for its further enhancement in biomedical horizon.<sup>28</sup> The addition of biopolymers improved the water retention and cellular proliferation properties of the hydrogels.<sup>29,30</sup> The poly(AAM)-based copolymers are highly swellable and mucoadhesive in nature.<sup>31</sup> Metronidazole is a widely used antibiotic drug against aerobic/anaerobic-related infections including various vaginal infections such as bacterial vaginosis. Its antimicrobial action is explained by its binding with microbial DNA and inhibits the synthesis of nuclear material, leading to cell death.<sup>32</sup>

The novelty of the present project relied on the fact that the innovative design of materials derived from carrageenan polysaccharide for use in VDD applications resolves health issues prevailing among women, especially those related to female genital health issues. This design involves the incorporation of tissue-like consistency, biocompatibility, mucoadhesion and vaginal fluid retention properties into the network structure, which are ideal requirements of biomaterials for use in vaginal drug delivery. These network hydrogels were fabricated *via* a copolymeric reaction of PVP and polyacrylamide onto CG to develop perfect biomaterials for VDD, which will also overcome the limitations related to the conventional vaginal DD dosages. Hence, proposed research work is based on the development of a functional material for the pharmaceutical evaluation of an antibiotic therapeutic agent.

## 2 Materials and method

### 2.1 Materials used

Iota-carrageenan [HiMedia Laboratories Pvt. Ltd], acrylamide [Merck specialties Pvt Ltd (Mumbai) India], PVP [Sigma-Aldrich Chemie GmbH], *N,N*-methylenebisacrylamide (NN-MBA) and ammonium persulfate (APS) [Fisher Scientific India Pvt Ltd, Mumbai, India] were materials used to design network hydrogels. Metronidazole was purchased from ALKEM laboratories Ltd Mumbai, India.

### 2.2 Synthesis of network polymeric hydrogels

Crosslinking reactions were envisaged to develop covalent linkages to form polymeric network hydrogels. The reaction was





Scheme 1 Pictorial representation of the synthesis and subsequent drug release from the hydrogel matrix.

initiated by adding the solution of a definite content of free radical initiator ammonium persulphate  $[APS] = 2.1 \times 10^{-2} \text{ mol L}^{-1}$  into a solution of definite content of CG = 10% w/v. Then, a definite amount of monomer  $[AAm] = 7.03 \times 10^{-1} \text{ mol L}^{-1}$ ,  $[PVP] = 3\% \text{ w/v}$  and cross linker  $[NN-MBA] = 6.40 \times 10^{-3} \text{ mol L}^{-1}$  were added to the reaction system. The process of crosslinking and polymerization was run for 3 hours for the completion of the reaction that formed insoluble crosslinked copolymeric materials and was assigned as CG-cl-poly(AAm)-PVP hydrogels or copolymers. Further, the optimization of various parameters were obtained by changing  $[AAm]$  from  $4.22 \times 10^{-1} \text{ mol L}^{-1}$  to  $12.63 \times 10^{-1} \text{ mol L}^{-1}$ ,  $[PVP]$  from 2% w/v to 5% w/v and cross linker from  $6.40 \times 10^{-3} \text{ mol L}^{-1}$  to  $32.43 \times 10^{-3} \text{ mol L}^{-1}$  during a copolymerization reaction. The optimized reaction parameters were obtained as  $[AAm] = 7.03 \times 10^{-1} \text{ mol L}^{-1}$ ,  $[PVP] = 3\% \text{ w/v}$ ,  $[NN-MBA] = 6.4 \times 10^{-3} \text{ mol L}^{-1}$ ,  $[CG] = 10\% \text{ w/v}$ ,  $[APS] = 2.1 \times 10^{-2} \text{ mol L}^{-1}$  based on swelling and structural consistency of hydrogels maintained after 24 h swelling. These optimized formulations were then employed for further investigations and subsequently utilized as matrices for sustained drug release and biomedical evaluations. A pictorial representation of synthesis and subsequent drug release from the hydrogel matrix is given in Scheme 1.

### 2.3 Characterizations

Polymer characterization was performed by various techniques using different analytic instruments. FESEM images and EDAX spectra were recorded using a JEOL-JSM6100 SEM, AFM analysis was performed using an INTEGRA, NT-MDT, Russia, FTIR spectra of the polymer sample were recorded using a BRUKER

ALPHA-Platinum-ATR-IR with KBr pellets, and  $^{13}\text{C}$ -NMR solid state of samples was recorded using a JEOL-ECZR600 NMR and XRD analysis was performed using a PAN-ANALYTICAL X'PERT PRO INSTRUMENT.

### 2.4 Physico-chemical and biomedical properties

**2.4.1 Swelling properties.** The swelling of copolymers was determined by the gravimetric method wherein dry polymer samples were weighed and immersed in a buffer solution. The samples were then removed from the solution periodically, wiped with tissue paper and weighed immediately to determine the swelling percentage with reference to their initial weight. The swelling of material was evaluated in a simulated vaginal fluid (SVF). Briefly, the SVF (pH 4.5) was prepared as described previously.<sup>33</sup> To 900 ml of distilled water, 3.51 g NaCl, 1.4 g KOH, 0.22 g  $\text{Ca}(\text{OH})_2$ , 0.018 g bovine serum albumin (BSA), 2 g lactic acid, 1 g acetic acid, 0.16 g glycerol, 0.4 g urea and 5 g glucose were added. These chemicals were stirred until complete dissolution. The pH of the mixture was then adjusted to 4.5 using HCl and the final volume was then adjusted to 1 L.

**2.4.2 Drug delivery properties.** Drug encapsulation in hydrogels was carried out by a swelling equilibrium method. For drug encapsulation, the sample was put in a drug solution of fixed concentration (metronidazole =  $500 \mu\text{g ml}^{-1}$ ) at  $37^\circ\text{C}$  for a specific time. The release of metronidazole from the encapsulated hydrogels was done by keeping the drug-containing sample in a solution of different pH release media. The drug loading and release of metronidazole were calculated from the calibration curves of metronidazole prepared in different media (distilled water  $\lambda_{\text{max}} = 319 \text{ nm}$ ), pH 2.2 buffer



( $\lambda_{\max} = 282$  nm), pH 4.5 buffer ( $\lambda_{\max} = 319$  nm) and pH 7.4 buffer ( $\lambda_{\max} = 318$  nm) using a UV spectrophotometer. The metronidazole release profile from various matrices was analyzed by applying Ritger and Peppas eqn (i):<sup>34,35</sup>

$$[(M_t/M_\infty) = kt^n] \quad (i)$$

where 'k' (polymer characteristic) and 'n' (diffusion exponent) are constants.  $M_t/M_\infty$  is a fraction of the drug released at time 't'. Release profile data were applied in various equations to find out the best fit kinetic model for the release of the drug from the drug-loaded sample.<sup>36,37</sup>

## 2.5 Biomedical properties

The blood compatibility of the material was assessed by examining the polymer interaction with citrated blood as thrombogenicity and haemolysis parameters.<sup>38–40</sup> The protein adsorption property of the hydrogels was determined using BSA as a reference protein by the Lowry method.<sup>41,42</sup> The antioxidant activity (AOX) of hydrogels was performed by 2,2'-diphenylpicrylhydrazyl (DPPH), Folin–Ciocalteu (FC) and phosphomolybdate (PM) reagent assays.<sup>43,44</sup> Mucoadhesion was determined by testing the detachment force required to separate the copolymer from the goat intestine membrane.<sup>45</sup> Cell viability assay for CG-cl-poly(AAm)–PVP was conducted by using a transformed cell line, namely RD (rhabdomyosarcoma cells obtained from the Central Research Institute, Kasauli-HP-India). The cytotoxic effect of the polymer sample was checked after treating cells (RD) with the polymer sample. The effect of polymer on RD cell lines (MTT Assay) was determined. The mean values of all measurements were used to calculate the cell viability percentage. The treated group of cells was compared with the control group in the absence of compounds.<sup>46</sup> The antimicrobial (AMI) properties of hydrogels were determined against bacteria *Pseudomonas aeruginosa* (*P. aeruginosa*), *Escherichia coli* (*E. coli*) and *Staphylococcus aureus* (*S. aureus*) by an agar well diffusion method. Agar spread Petri plates were used for this purpose. Prior to testing, nutrient broth, polymeric films and glass test tubes were sterilized in an autoclave at 121 °C and 15 lbs pressure for 24 h. The antimicrobial activity of biomaterials with and without the drug was evaluated by measuring the inhibition zone (in mm units) surrounding the polymer samples. The anti-inflammatory activity of the hydrogels was investigated by a technique that involves the inhibition of albumin denaturation, in which the samples' turbidity was measured at 660 nm.<sup>47</sup> The porosity of the hydrogels was obtained by the ethanol diffusion method.<sup>48</sup> The gel strength of the swollen hydrogels was determined using a texture analyser by recording the penetrating force required for the probe of instrument to insert into the hydrogel up to 3 mm depth.

## 3 Results and discussion

### 3.1 Characterizations

**3.1.1 FESEM.** FESEM analysis revealed a smooth and homogeneous morphology of sulphated polysaccharides, whereas a divergent irregular morphology of CG-PVP–

poly(AAm) hydrogels was observed during FESEM image assessment (Fig. 1). Irregular network structures appeared after the incorporation of poly(AAm)–PVP into the CG backbone *via* grafting and crosslinking reactions that led to the formation of a strong interconnected network developed as a result of covalent/non-covalent interactions between various functional moieties of CG-PVP–poly(AAm). These irregular networks appeared in the form of 3-D interconnected channels that are significant in controlling the swelling and drug release pattern of biopharmaceutical carriers. These interconnected channels appeared in the form of pores, enabling faster and extensive swelling of the polymer matrix, which is beneficial for hydrogels used in VDD carriers. The porous network structure of the hydrogel aids drug retention and facilitates slow DD to the vaginal site.<sup>49,50</sup> Varghese and coworkers<sup>51</sup> illustrated a porous 3-D interconnected microstructure of the CG-gelatin hydrogel that allowed easy flow of therapeutic agents and efficient nutrient transfer to the target site. Afloarea and coworkers<sup>52</sup> elucidated a sponge-like porous uneven morphology of chitosan hydrogels developed for the VDD of progesterone. From the FESEM images, Santo and coworkers<sup>53</sup> elucidated that the disorganized structures in CG-derived hydrogels were due to higher crosslinking in the network structure.



Fig. 1 FE-SEM images of (a) CG and (b) CG-cl-poly(AAm)–PVP polymer at different magnifications.



**3.1.2. 2EDAX.** Elemental analysis of CG-cl-poly(AAm)–PVP copolymer was performed to determine the elemental composition of samples (Fig. 2). The EDAX spectra illustrated the presence of carbon, hydrogen, sulphur and nitrogen elements in the obtained hydrogel-based VDD carriers. The ‘N’ and ‘S’ elements in hydrogels inferred the inclusion of CG, poly(AAm), PVP and NNMBBA crosslinker in the hydrogels on account of their copolymerization reaction. However, the elemental analysis results of dried samples showed only C, O and S in CG EDAX spectra. It appeared that amide moieties of poly(AAm), PVP and NNMBBA crosslinker introduced ‘N’ elements in the crosslinked product. Hassanzadeh-Afruzi and coworkers<sup>54</sup> found that the EDAX spectra of hydrogels shows the presence of nitrogen atoms after the incorporation of poly(AAm) into the CG backbone, confirming the successful modification of CG with poly(AAm).

**3.1.3 AFM.** The surface roughness evaluation of biomaterials from AFM analysis revealed the surface topography of the hydrogels. Both the average and the root mean square roughness were found to be 17.55 nm and 23.02 nm, respectively (Fig. 3). The roughness of the VDD carrier was owing to surface modulation by the copolymerization of poly(AAm)–PVP chains onto the sulphated polymer. The grafting reactions led to the formation of a crosslinked hydrogel network due to inter- and intra-cross-linking of polymer chains. These provide rough surface topography to the hydrogel, which is significant for VDD applications, as it increases the available surface area for the drug diffusion mechanism and, hence, prolongs the drug residence time. The uniform surface of PVP was modified into a rough and coarse surface due to the covalent bonding *via* the grafting reaction of poly(AAm).<sup>55</sup>

The surface roughness of VDD devices is a useful feature that provides adhesion properties to hydrogels. The mucoadhesion of VDD provides site-specific adherence of drug carriers to vaginal mucosa and releases the drug for a longer time period. The rough surface of the polymer increases the surface area



Fig. 3 AFM image of CG-cl-poly(AAm)–PVP polymers.

with mucosa and improves adhesion that leads to enhancement in therapeutic agent release from formulations.<sup>13</sup> Vaginal epithelium with a mucosal layer creates a protective barrier, wherein a rough hydrogel surface increases the contact area and enhances the interlocking of hydrogels with the mucosal layer. These rough surfaces deliver the drug site specifically in the vaginal region and prolong the diffusion time by releasing the drug slowly and gradually. Moreover, the vaginal fluid washes away smooth drug formulations, whereas a rough polymer surface promotes stronger adhesion to the vaginal membrane and prevents premature clearance of DD carriers.<sup>8</sup> The roughness of polymeric materials is also useful in improving biomedical applications, involving cell growth and cell proliferation during the healing of wounds. The surface roughness provides better adhesive property to the hydrogel, which provides stronger mucoadhesion of the hydrogel to the mucosal surface.<sup>56–58</sup> Overall, the roughness of the present hydrogels can enhance the mucoadhesive properties of site-specific DD formulations.

**3.1.4 FTIR spectroscopy.** Fig. 4 shows the FTIR spectra of the CG and CG-cl-poly(AAm)–PVP hydrogel. The FTIR spectra of CG revealed characteristic bands between 3251 and 3453  $\text{cm}^{-1}$

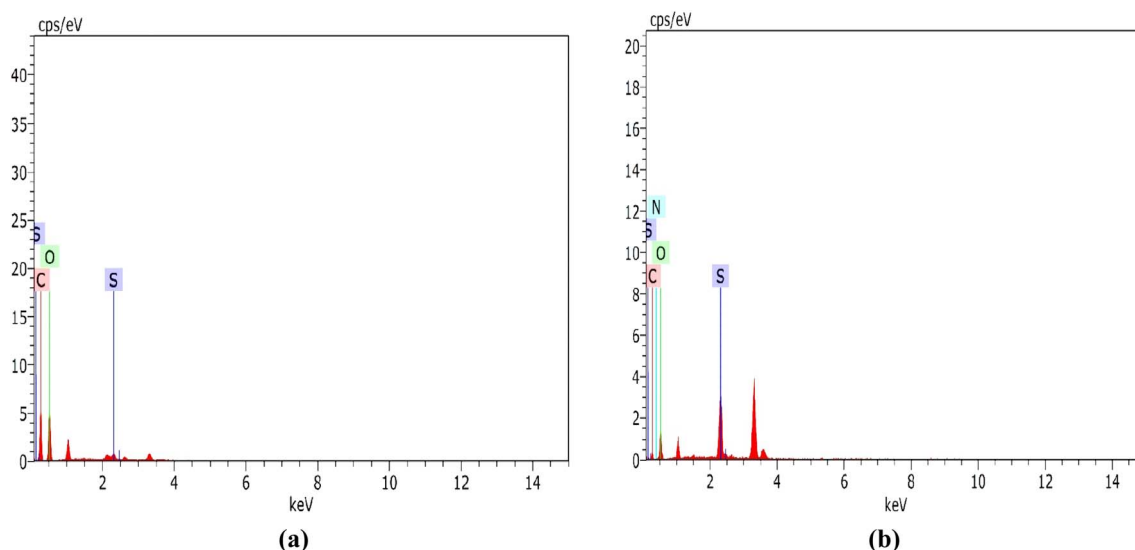


Fig. 2 EDAX images of (a) CG and (b) CG-cl-poly(AAm)–PVP polymer.





Fig. 4 FTIR spectra of (a) CG and (b) CG-cl-poly(AAm)-PVP polymers.

(ascribed to  $\text{-OH}$  stretching (str.)), at  $2961\text{ cm}^{-1}$  (due to  $\text{C-H}$  str.), at  $1269\text{ cm}^{-1}$  (due to sulfate ester ( $\text{O}=\text{S}=\text{O}$ ) symmetric str. of  $\text{S}=\text{O}$ ), at  $1150\text{ cm}^{-1}$  ( $\text{C-O}$  str.) and at  $1024\text{ cm}^{-1}$  ( $\text{C-O-C}$  str. of the glycosidic band present in CG). The characteristic bands of axial sulfate ester ( $\text{C-O-SO}_3$ ) were observed at  $844\text{ cm}^{-1}$  and  $806\text{ cm}^{-1}$  str. vibrations of O-4 of D-galactose-4-sulfate (G4S) and O-2 of D-galactose-2-sulfate (DA2S), respectively.<sup>59</sup>

The FTIR spectra of the hydrogel illustrated a band at  $3310\text{ cm}^{-1}$ , which was attributed to H-bonding in the network structure and a peak at  $2927\text{ cm}^{-1}$  was due to  $\text{-CH}_2$  str. of methyl and methylene groups of CG poly(AAm) and PVP. The band observed at  $1646\text{ cm}^{-1}$  (corresponding to  $\text{C}=\text{O}$  str. of amide I band of poly(AAm) and PVP), at  $1584\text{ cm}^{-1}$  (corresponding to N-H in-plane bending of  $\text{-CONH}_2$  of poly(AAm) as amide II),  $1410\text{ cm}^{-1}$  (due to the  $\text{-CH}_2$  bending vibrations of poly(AAm) and PVP), and at  $1284\text{ cm}^{-1}$  ( $\text{C-N}$  str. of  $\text{-CONH}_2$  of poly(AAm) as amide III and  $\text{C-N}$  vibration of PVP) of the polymer matrix.<sup>55,60</sup> The bands at  $1080$  and  $906\text{ cm}^{-1}$  are characteristic of galactopyranose ring/glycosidic linkage and  $\text{C-O}$  of 3,6-anhydrogalactose, respectively. The FTIR spectrum of the

copolymer indicated the incorporation of poly(AAm) and PVP into the CG backbone after the graft copolymerisation reaction. Similar diagnostic bands at  $840\text{ cm}^{-1}$  and  $850\text{ cm}^{-1}$  due to the axial sulfate ester ( $\text{C-O-SO}_3$ ) str. vibration of the G4S and DA2S units of CG, respectively, were reported in other research reports along with a band at  $1200\text{ cm}^{-1}$  due to the ester sulfate  $\text{O}=\text{S}=\text{O}$  symmetric vibration.<sup>61</sup>

**3.1.5  $^{13}\text{C}$  NMR.** The  $^{13}\text{C}$  NMR spectra of the CG and CG-cl-poly(AAm)-PVP hydrogels are presented in Fig. 5. The  $^{13}\text{C}$  NMR spectra of copolymers illustrated peaks between 184 and 175 ppm due to carbonyl carbon  $\text{C}=\text{O}$  of uronic acid of CG, poly(AAm) and (C-6) of the lactam group of PVP. The peaks between 60 and 103 ppm correspond to different carbon atoms of the pyranose ring of DA2S and G4S residues of CG. Peaks appeared around 40 ppm and between 30 and 35 ppm due to methine ( $\text{-CH}_2\text{-CHX-}$ ) and methylene ( $\text{-CH}_2\text{-CH}_2\text{-}$ ) of poly(AAm) and PVP. The peak at 40 ppm was also assigned to ring carbon ( $\text{-N-CO-CH}_2\text{-CH}_2\text{-}$ ) and 35 ppm to ring carbon ( $\text{-CH}_2\text{-C(H}_2\text{-N(C=O)-)}$ ) of the pyrrolidone ring of PVP. These peaks were found along with a sharp peak at 16 ppm corresponding to



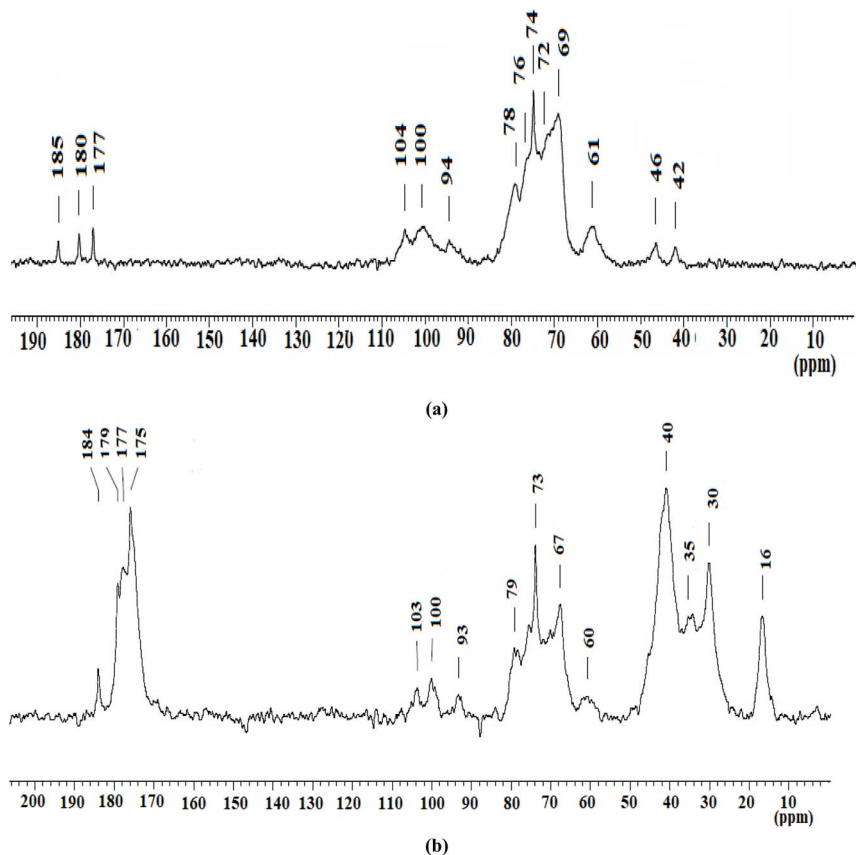


Fig. 5  $^{13}\text{C}$ -NMR of (a) CG and (b) CG-cl-poly(AAm)-PVP polymers.

methylene carbon ( $-\text{CH}_2-\text{CH}_2-\text{CH}_2-$ ) of the ring carbon of the pyrrolidone ring of PVP,<sup>55,62</sup> besides carbons of CG. The  $^{13}\text{C}$  NMR spectra of CG revealed peaks around 180 ppm because of the C=O carbon of uronic acid CG and at 104 ppm (anomeric C1), 69 ppm (C2), 76 ppm (C3), 72 ppm (C4), 74 ppm (C5) and 61 ppm (C6) due to the G4S residue of CG. The spectra also illustrated peaks at 94 ppm (C1), 74 ppm (C2), 76 ppm (C3 and C5), 78 ppm (C4) and 69 ppm (C6) DA2S unit residues of CG.<sup>63</sup>

Meena and coworkers<sup>64</sup> revealed that the  $^{13}\text{C}$  NMR spectra of the CG-poly(AAm) hydrogel showed peaks in the range of 180 ppm to 62 ppm of DA2S and G4S residues of CG, and diagnostic bands of poly(AAm) were observed in the range of 180 ppm of  $-\text{CONH}_2$ , 43 ppm of methine carbon and 35 ppm of methylene carbon of poly(AAm). Therefore, the presence of peaks in the range of 180 ppm confirmed the presence of C=O in PVP and poly(AAm), peaks at 40 ppm and 35 ppm confirmed the grafting of PVP and poly(AAm) onto the CG backbone. The absence of peaks in the range of 120–140 ppm due to the  $\text{sp}^2$  carbon atom of monomer ( $\text{CH}_2=\text{CH}-\text{X}$ ) of AAm indicated the conversion of  $\text{sp}^2$  hybridized carbon atom to  $\text{sp}^3$  carbon of polymer ( $-\text{CH}_2-\text{CH}-\text{X}-$ ).<sup>65</sup> Ammar and coworkers<sup>66</sup> showed presence of characteristic peaks at 177 ppm (due to C=O of PVP), at 44, 33 and 16 ppm (carbon of pyrrolidone ring ( $-\text{N}-\text{CO}-\text{CH}_2-\text{CH}_2-$ ), ( $-\text{CH}_2-\text{CH}_2-\text{N}-(\text{C}=\text{O})-$ ) and ( $-\text{CH}_2-\text{CH}_2-\text{CH}_2-$ ) respectively of PVP.

**3.1.6 XRD.** The XRD patterns of CG and CG-cl-poly(AAm)-PVP copolymers are shown in Fig. 6. The XRD patterns of CG showed sharp peaks at  $2\theta$  of  $9.44^\circ$ ,  $11.38^\circ$ ,  $17.84^\circ$ ,  $23.54^\circ$ ,  $28.19^\circ$ ,  $29.91^\circ$ ,  $31.2^\circ$  and  $40.5^\circ$ .<sup>67</sup> The presence of these intense peaks was due to orderly arranged polymeric chains of polysaccharides and inter- and intramolecular hydrogen bonding interactions among various functional groups present on saccharide units, which make CG crystalline. In the case of CG-PVP-poly(AAm) hydrogel, the presence of a broad peak near  $2\theta$  of  $22^\circ$  showed complete blending of synthetic polymers with the natural polymer CG. The introduction of these monomers *via* a polymerization reaction destruct hydrogen bonded interactions among the polymeric chains of saccharide units and reduces the ordered crystalline structure between CG polymeric chains. It led to a reduction in its crystallinity and the formation of short-range arrangement of polymeric chains, which endowed the amorphous character to the hydrogel that is useful in DD applications.<sup>68</sup>

Some degree of crystallinity of the material was modified after the inclusion of PVP and poly(AAm) in the CG backbone during copolymerization. This modulation in the long-range order of polymer chains is beneficial for the physico-chemical properties of the material, including sorption and drug release pattern. The amorphous structure of the hydrogel contains randomly arranged polymer chains that lead to the formation of a more open network structure that can accommodate a larger amount of drugs and, hence, improve the slow





Fig. 6 XRD patterns of (a) CG and (b) CG-cl-poly(AAm)-PVP polymers.

and controlled release of the drug from the hydrogel matrix.<sup>69</sup> Various other research reports also illustrated the modification of the crystalline structure of polysaccharides to short-range amorphous structures by destroying the H-bonded interaction in polysaccharides. Sutar and coworkers<sup>70</sup> observed a decrease in the crystallinity of pectin when modified with poly(AAm) due to a decrease in the intermolecular hydrogen bonded interaction between the polymer chains of the polysaccharide. These observations revealed that hydrogel-based VDD carriers are amorphous in nature, which is useful in the diffusion of solvent molecules during vaginal fluid uptake and release of drugs occurred in a slow manner. The reduction in crystallinity and the formation of a more amorphous state of materials enhance their ability for fluid sorption and drug delivery applications. It also promotes the flexibility and adaptability and enhances the functionality and long-term efficacy.<sup>71</sup>

### 3.2 Physico-chemical and biomedical properties

**3.2.1 Swelling analysis.** In order to modulate the degree of network density of hydrogel-based VDD formulations, the contents of AAm, PVP and NN-MBA were varied during their

synthesis, which was evaluated from the results of swelling properties (Fig. 7 and Table 1). The swelling results revealed that the increase in monomer content [AAm] from  $4.22 \times 10^{-1} \text{ mol L}^{-1}$  to  $12.63 \times 10^{-1} \text{ mol L}^{-1}$  led to a reduction in water uptake ability. Increase in poly(AAm) content in hydrogel resulted in formation of more compact network structure due to covalent linkage and intermolecular forces between polymer chains and thereby reduced hydrogels ability to absorb water.<sup>72</sup> Further, swelling first increased with the increase in PVP content from 2 to 4% w/v. The initial increase in the water absorption tendency of the hydrogel was due to the enhanced hydrophilicity of the gel matrix, which ultimately led to a greater swelling index. However, beyond 4% w/v concentration of PVP, there was a reduction in water uptake by hydrogels, which is due to the enhancement in compactness and network density that restricted polymer chain flexibility, resulting in a lower swelling ratio. With the increase in crosslinker NN-MBA content from  $6.4 \times 10^{-3} \text{ mol L}^{-1}$  to  $32.43 \times 10^{-3} \text{ mol L}^{-1}$  during synthesis, a decrease in swelling was observed due to the overall increase in aggregation and crosslinking density. The increase in the number of cross-linking points results in a denser structure due to the formation of polymer networks *via* the interaction of



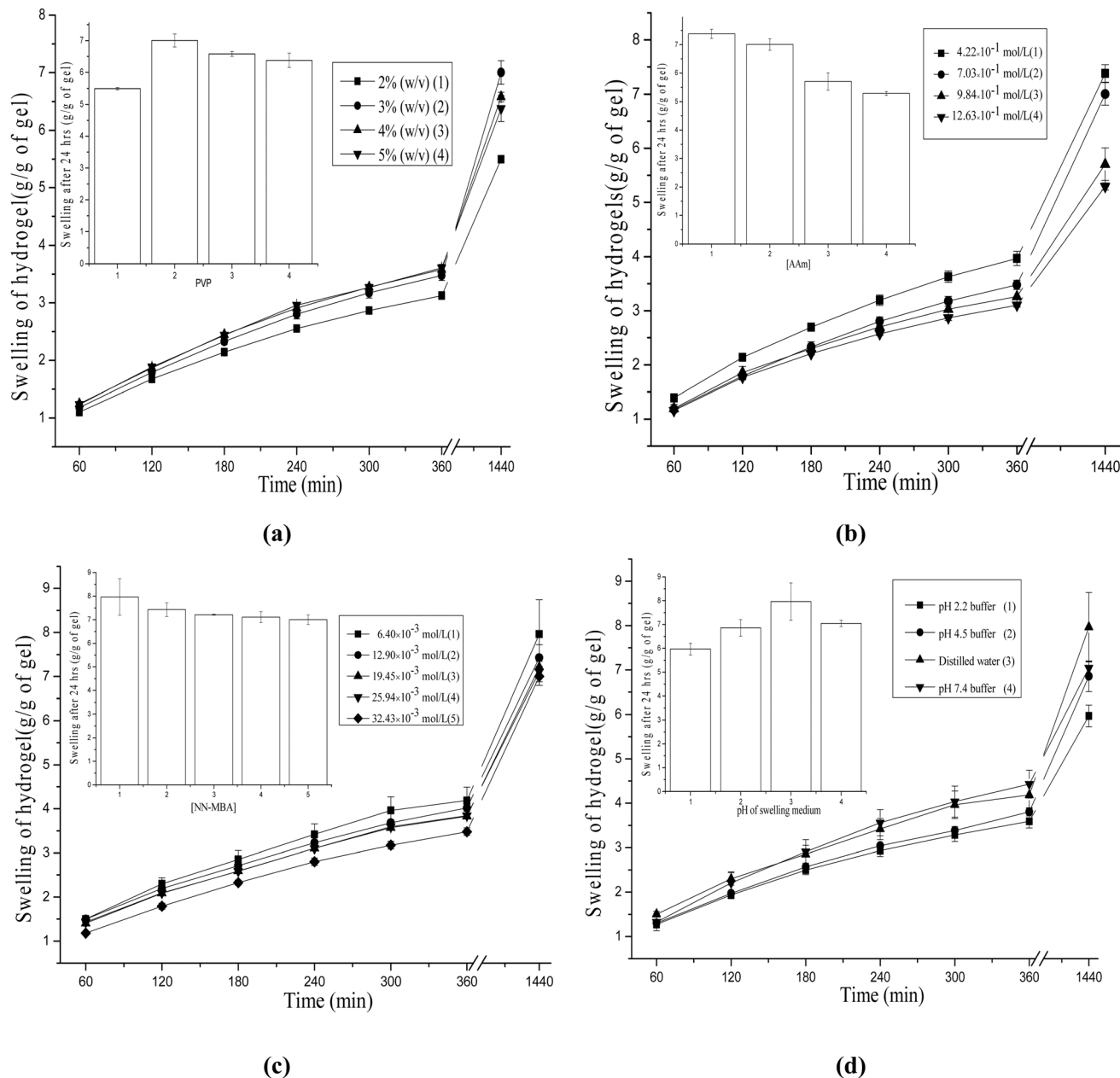


Fig. 7 Effect of (a) [AAm], (b) [PVP], (c) NN-MBA and (d) pH of swelling medium on the swelling of CG-cl-poly(AAm)-PVP hydrogels at 37 °C.

functional groups of CG, which can interact with the crosslinker that ultimately decreased the space and elasticity of the hydrogel network and restrict the movement and penetration of water molecules into polymer chains.

The swelling behaviour of the polymer matrix was further investigated in a different media including simulated gastric fluid (pH 2.2), SVF (pH 4.5), and simulated intestinal fluid (pH 7.4). The results demonstrated higher swelling at SVF than that at pH 2.2 and lower swelling than that at pH 7.4. Higher swelling at pH 7.4 might be due to the deprotonation or ionisation of polar functional groups that ionize and form charged zones on pendant polymer chains that lead to electrostatic repulsion between similar ionic charges in polymer chains and

forms loose polymer networks, resulting in higher water absorption and increased swelling.<sup>73</sup> Overall, the result of swelling analysis of hydrogel VDD properties revealed that physico-chemical properties of the hydrogel in terms of swelling were influenced by the content of the polymer used during grafting and crosslinking reactions, which gave the optimized parameters for designing of VDD formulations. At the same time, high degree of swelling was found in the SVF of pH 4.5, which further increased in a buffer solution of pH 7.4.

**3.2.2 Drug release properties.** The release profile of metronidazole drug from the CG-cl-poly(AAm)-PVP hydrogel was evaluated in a solution of varied pH buffer (Tables 2 and 3, Fig. 8). The diffusion of drug at pH 4.5 that mimics vaginal



**Table 1** Results of the swelling, gel strength, diffusion exponent '*n*', gel characteristic constant '*k*' and various diffusion coefficients for the swelling kinetics of CG-cl-poly(AAm)-PVP hydrogels

| S. no.  | Parameters      | Swelling after 24 h<br>(g g <sup>-1</sup> of gel) | Diffusion<br>exponent ' <i>n</i> ' | Gel characteristic<br>constant ' <i>k</i> ' × 10 <sup>2</sup> | Diffusion coefficients (cm <sup>2</sup> min <sup>-1</sup> ) |  |  |
|---|-----------------|---|------------------------------------|---|---|--|--|
|   |                 |   |                                    |   | Initial<br><i>D</i> <sub>i</sub> × 10 <sup>4</sup>          | Average<br><i>D</i> <sub>A</sub> × 10 <sup>4</sup> | Late time<br><i>D</i> <sub>L</sub> × 10 <sup>4</sup> |
| <b>Effect of PVP (% w/v)</b>                                  |                 |   |                                    |   |   |  |  |
| 1   | 2%              | 5.49 ± 0.03                                       | 0.58                               | 1.81  | 0.73  | 1.10   | 0.70   |
| 2   | 3%              | 7.01 ± 0.20                                       | 0.61                               | 138   | 0.60  | 0.87   | 0.59   |
| 3   | 4%              | 6.57 ± 0.08                                       | 0.59                               | 1.65  | 0.68  | 1.01   | 0.65   |
| 4   | 5%              | 6.40 ± 0.21                                       | 0.60                               | 1.62  | 0.77  | 1.10   | 0.73   |
| <b>Effect of [AAm] × 10<sup>1</sup> (mol L<sup>-1</sup>)</b>  |                 |   |                                    |   |   |  |  |
| 5   | 4.22            | 7.37 ± 0.16                                       | 0.58                               | 1.72  | 0.74  | 1.13   | 0.72   |
| 6   | 7.03            | 7.01 ± 0.20                                       | 0.61                               | 1.38  | 0.60  | 0.87   | 0.59   |
| 7   | 9.84            | 5.70 ± 0.30                                       | 0.56                               | 2.16  | 0.74  | 1.25   | 0.74   |
| 8   | 12.63           | 5.29 ± 0.06                                       | 0.55                               | 2.32  | 0.84  | 1.46   | 0.84   |
| <b>Effect of NN-MBA × 10<sup>3</sup> (mol L<sup>-1</sup>)</b> |                 |   |                                    |   |   |  |  |
| 9   | 6.40            | 7.96 ± 0.78                                       | 0.58                               | 1.75  | 0.69  | 1.08   | 0.69   |
| 10  | 12.90           | 7.42 ± 0.29                                       | 0.55                               | 2.06  | 0.72  | 1.20   | 0.74   |
| 11  | 19.45           | 7.21 ± 0.02                                       | 0.56                               | 1.89  | 0.70  | 1.13   | 0.71   |
| 12  | 25.94           | 7.11 ± 0.23                                       | 0.56                               | 2.00  | 0.72  | 1.17   | 0.73   |
| 13  | 32.43           | 7.01 ± 0.20                                       | 0.61                               | 1.38  | 0.64  | 0.93   | 0.63   |
| <b>Effect of swelling medium</b>                              |                 |   |                                    |   |   |  |  |
| 14  | pH 2.2 buffer   | 5.96 ± 0.24                                       | 0.58                               | 1.97  | 0.89  | 1.07   | 1.02   |
| 15  | pH 4.5 buffer   | 6.85 ± 0.34                                       | 0.59                               | 1.63  | 0.77  | 0.89   | 0.74   |
| 16  | Distilled water | 7.96 ± 0.78                                       | 0.58                               | 1.75  | 0.69  | 0.81   | 0.69   |
| 17  | pH 7.4 buffer   | 7.04 ± 0.13                                       | 0.68                               | 1.18  | 1.16  | 1.07   | 0.98   |

environment revealed more drug diffusion initially and then it followed a slow and prolonged pattern of drug release. The results of drug release suggest that metronidazole release from the hydrogel matrix were sustained at pH 4.5 within 24 hours. At pH 4.5, as the more compact structure and good porosity of the hydrogel matrix resulted in good control over drug release without dissolving at pH = 4.5. It is a matrix-based monolithic DD carrier, where the drug is uniformly infused and diffusion occurs uniformly due to swelling and solvent movement onto the hydrogel.

Various covalent and non-covalent interactions of the drug with various functional groups of the hydrogel matrix contributed to sustained drug release in SVF. In addition, the compact network structure and the porosity of hydrogel matrix contributed to slow diffusion of drug.<sup>74</sup> The degree of drug release from the hydrogel matrix mainly depends on the relative rate of diffusion of water molecules to the polymer network, swelling of hydrogel, rate of polymer chain relaxation and drug release profile.<sup>75</sup> In the present case, drug release from drug-infused hydrogels depends mainly on the swelling characteristics of the polymer matrix.

It implied that faster release during earlier stages was due to the rapid diffusion of surface-entrapped drugs from the biopolymer network when they come in contact with release media. After attaining a certain concentration, the swelling of a polymer network occurs and creates a matrix-like DD system, wherein the drug is uniformly distributed and drug diffuses

slowly, so that the drug release profile becomes smoother, and hence, more controlled and sustained drug release was observed.<sup>50</sup> Moreover, various types of covalent and non-covalent interactions of drugs with various functional moieties of hydrogel matrixes contribute to sustained drug release in the vaginal epithelium. Furthermore, the initial diffusion coefficient value ( $1.93 \times 10^{-4} \text{ cm}^2 \text{ min}^{-1}$ ) was higher than later stage diffusion coefficient values ( $1.75 \times 10^{-4} \text{ cm}^2 \text{ min}^{-1}$ ), indicating a slower and more controlled release over time. This initial phase with rapid drug release was then followed by a slower and more controlled release; with no burst effect due to reduction in concentration gradient, very less diffusion occurred, which was also reflected from the lower diffusion coefficient value.<sup>76</sup> The values of '*n*' suggested the non-Fickian diffusion mechanism of the drug. The *R*<sup>2</sup> values indicated that the kinetic model followed for release was the Hixson-Crowell model to describe the drug release profile of metronidazole.

Dubashynskaya and coworkers<sup>77</sup> have prepared a mucoadhesive system based on anionic sulfated polysaccharides for improved VDD of metronidazole with modified drug release profiles. The strong mucoadhesive character of the hydrogel was due to the entanglement of CG macro chains with glycoproteins in the mucosal membrane, resulting in sustained drug release.

In the research report of Sabbagh and coworkers,<sup>73</sup> the release of acyclovir from the poly(AAm)-based hydrogel for the treatment of vaginal infection was characterized at pH 4.2 and



Table 2 Results of diffusion exponent 'n', gel characteristic constant 'k', various diffusion coefficients and kinetic parameters for the drug release profile of metronidazole from drug-loaded CG-cl-poly(AAm)-PVP hydrogels

| Release medium  | Diffusion exponent 'n' | Gel characteristic constant 'k' × 10 <sup>2</sup> | Maximum amount of released drug, C <sub>max</sub> (mg L <sup>-1</sup> ) | Constant of the kinetic of release k <sub>rel</sub> × 10 <sup>5</sup> (s <sup>-n</sup> ) | Initial release rate r <sub>0</sub> (mg L <sup>-1</sup> s <sup>-1</sup> ) | Diffusion coefficients (cm <sup>2</sup> min <sup>-1</sup> ) |   |   |
|-----------------|------------------------|---|---|--|---|---|---|---|
|                 |                        |   |   |  |   | Initial (D <sub>i</sub> ) × 10 <sup>4</sup>                 | Average (D <sub>A</sub> ) × 10 <sup>4</sup> | Late time (D <sub>L</sub> ) × 10 <sup>4</sup> |
| pH 2.2 buffer   | 0.73                   | 1.33  | 166.11  | 1.57   | 0.43  | 2.41  | 1.09  | 2.53  |
| pH 4.5 buffer   | 0.74                   | 1.17  | 165.01  | 1.43   | 0.39  | 1.93  | 0.84  | 1.75  |
| Distilled water | 0.66                   | 2.06  | 109.769   | 3.33   | 0.40  | 2.20  | 0.83  | 2.79  |
| pH 7.4 buffer   | 0.79                   | 0.90  | 230.41  | 0.77   | 0.41  | 2.15  | 0.93  | 1.92  |

pH 7.4. They revealed that the faster release of the drug was observed initially in 1–2 h, followed by slow and sustained release up to 9 h. Narayana Reddy and coworkers<sup>78</sup> demonstrated that increasing the PVP content in the hydrogel matrix enhances hydrophilicity, leading to faster drug release. Higher PVP contents in chitosan–PVP microspheres also increase water uptake, resulting in greater cumulative drug release. Cirri and coworkers<sup>79</sup> also revealed that metronidazole release from the chitosan–alginate hydrogel involves an initial phase of rapid drug delivery from the hydrogel surface, followed by a slow and controlled diffusion phase, resulting in prolonged drug release. Sharifzadeh and coworker<sup>57</sup> revealed that the release of drug from the poly(AAm)–carboxymethyl cellulose hydrogel exhibited the initial release of drug due to the fast diffusion of drugs through pores present on the surface of the materials and then followed slower and prolonged release in SVF due to the formation of diffusion barriers in the hydrogel matrix. Healthcare products and DD devices besides being compatible with the vaginal pH should maintain their structural integrity for their restoration, as in the case of bacterial vaginitis. As per the WHO recommendation, the physiological vaginal pH (3.5–4.5) plays an important role and a change in pH can be dangerous.<sup>80</sup>

Additionally, a study was conducted in distilled water and pH 2.2 and pH 7.4 buffer media in order to observe the diffusion characteristics of the polymer matrix in buffer solutions to expand their future applications in designing DD systems for the gastrointestinal tract. Furthermore, various enzyme immobilization and tissue engineering applications were evaluated in pH 7.4 buffer media, wherein this matrix could be explored as a material for advanced applications.

A pictorial representation of the mucoadhesive polymer–drug interactions for metronidazole drug delivery is shown in Scheme 2.

### 3.2.3 Blood compatibility

**3.2.3.1 Haemolytic and thrombogenicity assay.** Haemolytic and thrombogenicity assays of VDD formulations were performed as the biopharmaceutical characterization of materials to determine their blood compatibility properties (Table 4). These properties displayed compatibility features during their interactions with blood. The analysis of these tests disclosed that the thrombogenicity of materials was  $82.96 \pm 1.67\%$  and the haemolytic index value was  $1.35 \pm 0.13\%$  during blood–polymer interactions. The material expressed haemolysis to a lower extent, indicating the less RBC rupturing tendency of hydrogels. These results indicated that polymer samples possess a non-haemolytic and non-thrombogenic character. Therefore, these biomaterials hold potential for use in biomedical or clinical applications, including VDD.

The blood compatibility features of hydrogel–VDD formulations were attributed to their hydrophilic nature. The presence of polar functional groups (SO<sub>3</sub>H–OH, –C=O, and –CONH<sub>2</sub>) in the hydrogel surface does not allow polymers to sufficiently interact with the erythrocytes due to the formation of a hydrated layer barrier *via* electrostatic repulsive forces, thereby preventing the disruption of their membrane. CG provides excellent blood compatibility owing to its sulfate groups. Various sulfate groups interact with blood factors to inhibit coagulation



**Table 3** Results of correlation coefficients ( $R^2$ ) of different drug release models for the release profile of metronidazole drug-loaded CG-cl-poly(AAm)-PVP hydrogels

|                  |  | Drug release mediums |               |                 |               |
|------------------|--|----------------------|---------------|-----------------|---------------|
|                  |  | pH 2.2 buffer        | pH 4.5 buffer | Distilled water | pH 7.4 buffer |
| Zero order       | $R^2$  | 0.93                 | 0.96          | 0.90            | 0.96          |
|                  | $K_o \times 10^3$ ( $\text{min}^{-1}$ )      | 2.20                 | 2.00          | 2.10            | 2.20          |
| First order      | $R^2$  | 0.98                 | 0.99          | 0.99            | 0.98          |
|                  | $K_1 \times 10^3$ ( $\text{min}^{-1}$ )      | 7.42                 | 5.72          | 8.76            | 6.55          |
| Higuchi          | $R^2$  | 0.98                 | 0.99          | 0.97            | 0.99          |
|                  | $K_H \times 10^2$ ( $\text{min}^{-1/2}$ )    | 6.03                 | 5.69          | 5.97            | 6.13          |
| Korsmeyer-Peppas | $R^2$  | 0.97                 | 0.98          | 0.96            | 0.99          |
|                  | $K_{KP} \times 10^2$ ( $\text{min}^{-n}$ )   | 1.33                 | 1.17          | 2.06            | 0.90          |
| Hixson-Crowell   | $R^2$  | 0.99                 | 0.99          | 0.99            | 0.99          |
|                  | $K_{HC} \times 10^3$ ( $\text{min}^{-1/3}$ ) | 1.59                 | 1.33          | 1.75            | 1.49          |

pathways, thereby preventing thrombus or clot formation.<sup>81</sup> At the same time, present materials are composed of CG, PVP and poly(AAm), which are hydrophilic and have also been reported as blood compatible in nature in other research reports. Popov and coworkers<sup>82</sup> revealed that the inclusion of CG onto pectin has induced negligible erythrocyte haemolysis and caused no change in their morphology. The rise in poly(AAm) content in chitosan-hydrogels has reduced haemolysis, attributed to their surface composition that provided minimum interaction with blood cells. The poly(AAm)-based hydrogel illustrated negligible clot formation and revealed the antithrombogenicity character of the materials.<sup>72</sup> PVP copolymers did not express any significant haemolytic effect on RBCs due to the negative surface charge and hydrophilicity that supported their suitability as DD carriers.

Overall, sulphated amide-containing CG hydrogels are biocompatible and show potential as materials for VDD carriers. The biocompatibility and tolerability of various components of DD formulations are the main requirements when VDD formulations are employed for the treatment of microbial or viral pathologies associated with the mucosal lesions associated with the damage of the mucosal membrane.

**3.2.3.2 Protein adsorption.** The protein adsorption tendency of the hydrogel was investigated using BSA, and the results are demonstrated by the content of protein adsorbed onto the polymer surface. The CG-cl-poly(AAm)-PVP hydrogel showed  $3.31 \pm 0.18\%$  BSA adsorption after 24 hours of incubation at 37 °C (Table 4). Protein adsorption indicates the compatibility feature of materials with biological systems when employed in biomedical uses. In the present case, BSA interactions with the hydrogel showed a minimal amount of protein adsorption onto their surface due to the strong hydration ability of the hydrogel layers. It has been found that during the interaction of material surfaces with blood, a series of biochemical reactions occur that lead to the activation of the blood clotting process. The super-hydrophilic layer formed on a hydrated polymer surface repels negatively charged plasma proteins and resists platelet adhesion, thereby preventing thrombus formation. This also demonstrates the biocompatibility properties of hydrogels. Hence, these hydrogels could be employed for the delivery of

therapeutic agents as efficient VDD carriers. The hydrophilic nature of materials was owing to CG, PVP and poly(AAm). CG has been found to reduce protein adsorption in many reports.<sup>37,72</sup> Tavakoli and coworkers<sup>83</sup> revealed that the inclusion of CG in starch increased the hydrophilic character, reduced the adherence of BSA molecules onto the gel surface and improved blood compatibility of the hydrogel. The presence of sulfated galactan created a negative surface that restricts BSA adsorption on the hydrogel surface *via* electrostatic repulsions operating between the hydrogel and the blood surface, which has been considered as a reason for lower protein adsorption and better compatibility properties.<sup>84,85</sup> The inclusion of PVP chains has improved the blood compatibility of the polymer matrix. The improved anti-protein adsorption property was due to the increase in hydrophilicity and also electrostatic repulsions operating between the modified polymer surface and proteins, which decreases the amount of protein adsorption to the polymer surface and improves blood compatibility.<sup>86</sup>

**3.2.4 Antioxidant (AOX) activity.** The AOX potential of hydrogels was analyzed by three different AOX activity assays: DPPH, FC, and PM reagent assays (Table 4).

**3.2.4.1 DPPH reagent assay.** The AOX power of the hydrogel was determined by the DPPH test, wherein the hydrogels exhibited  $52.40 \pm 1.14\%$  scavenging ability. The DPPH method was employed to evaluate the antioxidant activity based on spectrophotometric determination *via* the hydrogen atom transfer mechanism. Hydrogels act as antioxidants, as they can interact and inhibit the initiation and propagation of oxidizing chain reactions that are generated by reactive free radicals before it causes damage to organs. They inhibit free radical reactivity by the donation of a hydrogen atom from the hydroxyl groups present in polysaccharide chains. This method is based on the reduction of violet DPPH radicals by antioxidants *via* a hydrogen atom transfer mechanism to cause a change in colour to a pale yellow DPPH molecule.<sup>87</sup> Due to the presence of a higher number of active hydroxyl groups in the polymer chains, CG showed high radical scavenging activity by the H-abstraction reaction with free radicals.<sup>88</sup> Madruga and coworkers<sup>89</sup> revealed that various sulfated, acetylated or phosphorylated derivatives of CG exhibit antioxidant characteristics





Fig. 8 Release profile of metronidazole from drug-loaded CG-cl-poly(AAm)-PVP polymers in different media at 37 °C.

by scavenging superoxide, hydroxyl and DPPH radicals due to their strong hydrogen-donating ability.

**3.2.4.2 FC reagent assay.** The F-C method confirmed the AOX activity of the hydrogel. The polymer sample revealed an AOX of  $21.52 \pm 0.71$   $\mu\text{g}$  equivalent of gallic acid (GAE) in the F-C reagent assay. The polyphenolic compounds have direct correlation with AOX, wherein polyphenols due to their hydroxyl groups possess free radical scavenging ability.<sup>90</sup> In the F-C reagent assay, phosphomolybdic acids and phosphotungstic acids present in the F-C reagent react with various antioxidants present in polysaccharides to form chromogens.<sup>91</sup>

**3.2.4.3 PM assay.** The PM assay is a quantitative method that gives direct estimation of the reducing ability of hydrogels. The biomaterial revealed an AOX activity of  $447.81 \pm 15.08$   $\mu\text{g}$  equivalent of ascorbic acid (AAE) in the PM assay. The total antioxidant capacity or reducing power of hydrogels is based on their ability to donate electrons from antioxidants to unstable Mo(vi) complexes and subsequently form a green-coloured Mo(v) complex at acidic pH values.<sup>92</sup> Ferreira and coworkers<sup>93</sup> found that poly(AAm)-derived hydrogels exhibited AOX capacity illustrated by the PM assay for the treatment of wound lesions.

Overall, these three assays of AOX activity measurement demonstrated the AOX nature of biomaterials, which could be beneficial in VDD. Various types of vaginal infections lead to oxidative stress that creates an imbalance between free radicals and antioxidants. Excessive ROS production causes damage to healthy tissues and disrupts the cell membranes, which ultimately contributes to tissue inflammation.<sup>94</sup> Antioxidants neutralize these free radicals by donating electrons or hydrogen-free radicals, thereby stabilizing these reactive molecules. This process helps in preventing cellular and tissue damage and protects against inflammatory responses.

The hydrogel reduces oxidative stress that drives the inflammatory response. Vaginal infections often disturb the balance of the vaginal microbiome, leading to the overgrowth of harmful bacteria or fungi.<sup>95</sup> This imbalance triggers inflammation as the body attempts to eliminate excess pathogens. By creating a healthier, less inflamed environment, the hydrogel supports the growth of beneficial lactobacilli, helping to restore the vaginal microbiome balance.<sup>96</sup> A balanced microbiome is less susceptible to recurrent infections and inflammation. Hence, the AOX properties of VDD carriers may also be responsible for the reduction in inflammation occurring in the vaginal mucosa. ROS scavenging biomaterials alleviate inflammation by directly or indirectly balancing the production and elimination of ROS.<sup>97</sup> Some natural polysaccharides can act as ROS scavengers by protecting against oxidative damage in inflammatory diseases. It is the hydroxyl groups in the polymer matrix, which transfer one 'H' atom or a single electron to ROS, stabilizing reactive species, chelate metal catalysts, activate antioxidant enzymes, and inhibit oxidases. ROS scavenging by biomaterials also limits inflammation and protects the host from damage.<sup>98-100</sup> A pictorial representation of hypothetical free radical scavenging of DPPH by hydrogels is illustrated in Scheme 3.

**3.2.5 Mucoadhesion.** Mucoadhesive characterization of the material was assessed by measuring the detachment force and work of adhesion necessary to detach the hydrogel from a goat's biological membrane. Mucoadhesion analysis of biomaterials illustrated that these polymeric VDD formulations required a force of  $93 \pm 6.11$  mN for separation from the biological membrane that needed  $0.09 \pm 0.02$  N mm work of adhesion (Table 4). These results highlight the mucoadhesive feature of hydrogel, a vital requirement of VDD devices to improve drug retention and efficacy by prolonging the residence time of





Scheme 2 Pictorial representation of mucoadhesive polymer–drug interactions for metronidazole drug delivery.

delivery vehicles in the vaginal environment. It provides information regarding site-specific drug delivery from polymeric patches containing bioactive therapeutic agents for the treatment of problems associated with the vaginal region.<sup>15</sup> Mucoadhesive polymers are utilized in the formulation of VDD carriers for drug release through attachment to vaginal mucosa, where the drug diffuses from the polymeric gel to the mucosal epithelium. Vaginal environment including vaginal secretions, along with the mucoadhesion properties of the DD device, plays an important role in controlling drug diffusion from DD systems. It prolongs the drug residence time of medical devices on vaginal mucosa, which provides the desired concentration needed for the specific bio-therapeutic response of the active drug for efficient treatment of the associated problems of the vaginal region.<sup>17</sup>

Overall, the results indicated that the mucoadhesive hydrogel dressing impregnated with the drug could be explored for site-specific treatment of vaginal infections, inflammations, parturition, *etc.* It provides adhesion to vaginal mucosa, where the fluid helps in the diffusion of the drug from the VDD carrier

and can maintain the drug concentration at the target site. Various DD formulations are available for treating vaginal infections. However, mucoadhesive polymer-derived VDD carriers are advantageous over conventional formulations in terms of mucoadhesiveness, drug residence time, *etc.*, which reduce the drug diffusibility of conventional formulations.

The adhesive properties of hydrogels were due to electrostatic interactions among the functional groups of various constituents of hydrogels and the functional groups of the mucosal membrane. Hydrogels are composed of CG, PVP and poly(AAm), which are hydrophilic in nature and are capable of providing various covalent and non-covalent interactions with glycoproteins of mucin of the membrane, and these materials have been reported to exhibit mucoadhesive property.<sup>101</sup> The CG itself exhibits the bio-adhesive character due to the presence of abundant H-bond forming groups, which interact with the mucosal membrane, leading to significant prolongation of the drug residence time of VDD carriers and enhanced therapeutic effectiveness.<sup>102</sup>





Scheme 3 Pictorial representation of hypothetical free radical scavenging of DPPH by the hydrogel matrix.

Pacheco-Quito and coworkers<sup>103</sup> found prolonged drug residence time and controlled release of acyclovir from CG-based mucoadhesive vaginal tablets *via* adhesive mechanisms

mediated by hydrogen bonds and electrostatic interactions with the mucosal membrane. The hydrophilic nature of poly(AAm) and PVP also enhances their ability to form strong H-bonds with

the wet surface of the mucosal membrane. The mucosal membrane comprises mucus that is composed of mucin, which acts as an anionic polyelectrolyte due to the presence of sulfate groups and sialic acid.<sup>101</sup> When the polymer comes in contact with the mucosal surface, interpenetration and interlacing of the mucoadhesive polymer chain with mucosal glycoprotein occur by forming various covalent and non-covalent bonds.<sup>104</sup> Sánchez-Sánchez and coworkers<sup>105</sup> have found that the inclusion of CG into the hydrogel increases the adhesive properties of the CG-based hydrogel. Moreover, the addition of binders such as PVP into the polymer produces compacted granules that remain adhered to the vaginal mucosa, regardless of the formulation composition or the pH of the medium (pH 4.5). Van der Bijl and coworkers<sup>106</sup> revealed that the permeability of vaginal mucosa is similar to buccal mucosa, but in comparison to intestinal and colonic mucosa, its permeability was higher. Tugcu-Demiroz and coworkers<sup>107</sup> have prepared metronidazole-loaded PVP-based formulations for treating bacterial vaginosis.

The adhesiveness of formulations improved with the increase in the PVP content due to intermolecular H-bonded interactions between PVP and mucin, suggesting its prolonged residence in the vagina. A pictorial representation of hydrogel adhesion to the mucosal membrane is shown in Scheme 4.

**3.2.6 Cell viability assay.** The impact of the hydrogel on the cell viability of transformed RD cells demonstrated  $190 \pm 7.07\%$  cell viability upon exposure to biomaterials (Table 4). The cell viability assay indicated that CG hydrogels showed excellent cyto-compatibility and non-cytotoxicity to mammalian cells. Instead, the samples promote the proliferation of cells and materials that may help in damaged tissue regeneration and ensure the proper functioning of the vaginal tissue, especially when these tissues are compromised by inflammation or infections.<sup>28</sup> The results are in accordance with the ISO standard,<sup>108</sup> and these hydrogels are considered non-toxic. Therefore, it can be assumed that the hydrogel coating does not have a toxic effect on cells upon contact with materials. Hence,



Scheme 4 Pictorial representation of hydrogel adhesion to the mucosal membrane.



**Table 4** Results of thrombogenicity, haemolytic potential, mucoadhesion, antioxidant activity, cell viability, anti-inflammatory activity, gel strength and porosity of CG-cl-poly(AAm)-PVP hydrogels

| Properties                     | Thrombogenicity            | Inference                |
|--------------------------------|----------------------------|--------------------------|
| Thrombogenicity percentage (%) | 82.96 ± 1.67%              | Non-thrombogenic nature  |
| Haemolytic index (%)           | 1.35 ± 0.13%               | Non-haemolytic nature    |
| Protein adsorption (%)         | 3.31 ± 0.18%               | Biocompatible nature     |
| <b>Mucoadhesion</b>            |                            |                          |
| Peak detachment force (mN)     | 93 ± 6.11 mN               | Mucoadhesive nature      |
| Work of adhesion (N mm)        | 0.35 ± 0.03 N mm           |                          |
| <b>Antioxidant activity</b>    |                            |                          |
| F-C reagent assay              | 21.52 ± 0.71 µg GAE        | Antioxidant nature       |
| Phosphomolybdenum assay        | 447.81 ± 15.08 µg AAE      |                          |
| DPPH reagent assay             | 52.40 ± 1.14% inhibition   |                          |
| Cell viability test            | 190 ± 7.07% cell viability | Cyto-compatible nature   |
| Anti-inflammatory properties   | 4.49 ± 0.08%               | Anti-inflammatory nature |
| Porosity                       | 47.9 ± 1.32%               | Porous nature            |

polymeric materials did not exert a negative impact on cell viability and did not pose a substantial cytotoxicity risk to mammalian cells. Therefore, these hydrogels could be considered as promising candidates for various biomedical applications. Overall, the dressing materials exhibited nontoxic and biocompatible features, which are suitable for biomedical applications.

The cell viability properties of the materials may be due to the composition of hybrid materials. CG-derived materials demonstrated a cyto-compatible nature during the cell proliferation test, and the morphology of cells remains unaffected and the nuclei of cells retained the round morphology.<sup>109</sup> Ashe and coworkers<sup>110</sup> revealed the cell viability of cryo-preserved cells in porous CG-gelatine hydrogels. After the incorporation of growth factors in the hydrogel, osteogenic cell proliferation and attachment improved. The chitosan-poly(AAm)-based hydrogel test sample showed no toxicity towards fibroblast cells.<sup>72</sup> The carboxymethyl cellulose-poly(AAm)-based hydrogel in the MTT assay revealed low cytotoxicity toward human skin fibroblasts.<sup>57</sup> The results of cell viability tests indicated that the present CG-based material is suitable and safe for VDD formulations.

**3.2.7 Antimicrobial (AMI) activity.** The AMI efficacy of blank and metronidazole-integrated network gels was evaluated by exposing the materials to Gram-negative (*P. aeruginosa* and *E. coli*) and Gram-positive (*S. aureus*) bacterial strains during the AMI test (Fig. 9). The evaluation involved measuring the diameter of the inhibition zone formed around disc samples, which indicated their AMI potency. The material exhibited a negligible zone of inhibition in the blank sample in comparison to the antibiotic impregnated formulation. This zone of inhibition is directly linked to the AMI behaviour of the sample analyzed. The hydrogel matrix revealed a zone of inhibition of 2.02 ± 0.01 mm against *S. aureus* and did not show any AMI activity against Gram-negative bacteria (*P. aeruginosa* and *E. coli*). However, drug-incorporated hydrogels displayed a zone of inhibition of 13 mm, 4 mm and 15 mm against respective

bacterial strains, highlighting their enhanced AMI effect compared to the hydrogel without any drug. It may be owing to the antibiotic drug present in the hydrogels.

Khade and coworkers<sup>111</sup> have developed metronidazole integrated formulations (gelatine-PEG) for VDD for the treatment of bacterial vaginosis, and the materials have been found to exhibit effective AMI activity against *E. coli* and *B. subtilis*. The AMI efficiency of metronidazole-loaded hydrogels was tested against *E. coli*, which is predominant in bacterial vaginosis. Permana and coworkers<sup>112</sup> revealed that due to the ability of gel flakes to localize metronidazole in the vaginal tissue, it was confirmed that this system could show significantly higher antibacterial activities in the bacterial vaginosis model. Some degree of AMI activity was due to sulphated CG polysaccharides in hydrogel samples, which fight against the bacterial strains by binding to the glycoprotein receptors present on the bacterial cell surface. This interaction leads to the disruption of the bacterial membrane and increases the permeability of the cytoplasmic membrane, protein leakage, and ultimately death of the microorganism.<sup>113</sup>

**3.2.8 Anti-inflammatory activity.** The anti-inflammation activity test of hydrogels revealed that the material did not exert any anti-inflammatory effect. This test is based on the ability of materials or extracts or chemicals to inhibit protein denaturation. The results of this test illustrated that the hydrogels were able to inhibit only 4.49 ± 0.08% of BSA protein denaturation as compared to a standard, which was an anti-inflammatory drug, sodium diclofenac (75 µg ml<sup>-1</sup>), that showed 17.25 ± 0.12% inhibition of BSA protein denaturation. These results indicated that CG-based hydrogels themselves do not possess any anti-inflammatory characteristics. A small anti-inflammatory action may be due to its ability to exhibit the antioxidant activity that prevents cells from oxidative stress and subsequently inhibits inflammation of tissues. In the denaturation process, proteins lose their tertiary and secondary structures due to external stress in the form of heat. This denaturation of proteins causes inflammation.<sup>114</sup> The anti-





Fig. 9 Antimicrobial activity of (a, c and d) CG-cl-poly(AAm)-PVP and (b, e and f) drug metronidazole-loaded copolymers against *P. aeruginosa*, *E. coli* and *S. aureus*.

inflammatory activity of CG-based hydrogels was evaluated by using inhibition of albumin denaturation. Inflammation is a biological response of the body against aggressive agents such as irritants, pathogens or damaged cells. Generally, various causing agents bring inflammation to the vaginal region, including vaginal infections (STD and UTI), hormonal changes, allergic reactions and physical stresses. These factors disrupt the natural balance of vaginal flora and result in irritation, dryness and thinning of vaginal tissues, making them prone to inflammation. Hence, the use of anti-inflammatory reagents is essential in managing vaginal inflammation to restore the natural balance in the vaginal environment.<sup>115</sup> Overall, it has been inferred that the present VDD formulations itself cannot

exert any anti-inflammatory effect during their application to the vaginal region.

**3.2.9 Porosity.** The porosity of the biomaterial was found to be  $47.9 \pm 1.32\%$  based on the results of the porosity test conducted on the sample (Table 4). The results indicated the porous characteristics of polymers, highlighting their ability to absorb a significant amount of solvent. This may be due to the formation of structurally crosslinked hydrophilic polymers through the crosslinked reaction of poly(AAm)-PVP onto the CG backbone. These interconnected pores or channels provide a larger surface area for drug loading and controlled release of therapeutic agents. The high porosity of hydrogels facilitates swelling, and exchange of nutrients, oxygen and waste



products.<sup>116</sup> Porous hydrogels impregnated with drugs ensure a slow and sustained drug release for the prolonged therapeutic action at the vaginal site without affecting the vaginal microbiome.<sup>117</sup> Besides application in VDD, they are extensively used in wound dressings. These porous hydrogels with high-interconnected porosity enable cell attachment, migration and proliferation for the regeneration of the skin. It also prevents tissue from dehydration and keeps a moist environment at the wound site, enhancing angiogenesis and collagen synthesis.<sup>118</sup>

**3.2.10 Gel strength.** The results of gel strength of hydrogels were found to be the reverse of swelling trends of hydrogels. The gel strength of CG-cl-poly(AAm)–PVP hydrogels was evaluated as a function of change of [AAm] from  $4.22 \times 10^{-1} \text{ mol L}^{-1}$  to  $12.63 \times 10^{-1} \text{ mol L}^{-1}$ , [PVP] from 2% w/v to 4% w/v and [NN-MBA] from  $6.40 \times 10^{-3}$  to  $32.43 \times 10^{-3} \text{ mol L}^{-1}$ . With the increase in [AAm] concentration, the gel strength increased due to the formation of denser polymer networks of hydrogels. With the increase in PVP concentration, the gel strength first decreases due to more swelling and expansion of the hydrogel network and then decreases due to a decrease in swelling. An increase in crosslinker content during the formation of hydrogel enhances the tensile properties of the materials due to the enhancement in crosslinking density in polymers. An increase in the pH of the swelling medium influenced the gel strength of hydrogels. However, the gel strength reduced with a rise in the pH of swelling medium due to the increase in the swelling and expansion of the hydrogel networks.<sup>119,120</sup>

Overall, CG in the DD systems has induced blood compatibility, antioxidant and bioadhesion features to the drug delivery carrier. The inclusion of drug metronidazole in CG-based VDD carriers has provided sustained release from hydrogels. Direct use of metronidazole whether administered orally or topically is often associated with several side effects including gastrointestinal disturbances and vaginal irritation. These adverse effects limit the therapeutic efficacy of the drug. Entrapping metronidazole within the hydrogel matrix offered an advanced controlled, site-specific, localized drug delivery, reducing the side effects of market-available metronidazole formulations. Brandt and coworkers<sup>121</sup> further supported this fact and found that the intravaginally applied metronidazole drug was more effective relative to the orally applied drug in the treatment of bacterial vaginosis, and the intravaginally applied drug simultaneously exhibited significantly less side effects. Permana and coworkers<sup>122</sup> developed mucoadhesive chitosan–gellan gum-based hydrogels for treatment of bacterial vaginosis. These metronidazole-loaded gel flakes showed a sustained release pattern over an extended period. This was attributed to the strong adhesion of the hydrogel, which allowed it to remain in contact with the vaginal tissue for over 8 hours, and hence facilitated the continuous release of metronidazole that effectively reduced the viability of *E. coli* and *S. aureus* bacterial strains, thereby promoting the faster healing of vaginal tissue. Recently, the CG-based hydrogel has also been explored by Thakur and Singh<sup>123</sup> for its application in pH-sensing colonic drug delivery for sustainable development. However, abiotic synthetic receptors by imprinting the surface marker have also been designed, which is a new era of drug design and discovery. The synthetic receptors

have been designed by molecular imprinting for use in the surface marker of bacterial strain and selective binding of bioactive oligosaccharides to increase the efficacy of drug molecules.<sup>124,125</sup> This approach is a future prospectus in this area of research, which could be explored for VDD.

## 4 Conclusions

The physico-chemical parameters in terms of swelling demonstrated that crosslinking in network hydrogels could be modulated as per requirement of VDD carriers by varying the monomer and crosslinked content during the synthesis of hydrogels, which gave the optimized parameters for the designing of VDD formulations. The FESEM and AFM characterizations of hydrogels revealed their heterogeneous morphology with roughness in surface, significant for better adhesion to the mucosal membrane. FTIR and <sup>13</sup>C NMR spectroscopic analysis confirmed the successful incorporation of poly(AAm) and PVP into CG. One gram of hydrogel absorbed approximately seven grams of simulated vaginal fluid. Hydrogels expressed  $190 \pm 7.07\%$  viability for RD cells and promoted their proliferation, which signified their non-toxic nature to the mammalian cell. Hydrogel exhibited non-haemolytic features revealed from  $1.35 \pm 0.13\%$  haemolytic index value. Hydrogels depicted  $52.40 \pm 1.14\%$  scavenging ability against DPPH radicals that outlined their antioxidant characteristic. The mucoadhesive performance of materials was expressed from the fact that it required a force of  $93 \pm 6.11 \text{ mN}$  for its separation from the mucosal surface. Additionally, the diffusion of antibiotic agents from the drug-infused hydrogel followed a non-Fickian diffusion mechanism, and the release profile was best interpreted by the Hixson–Crowell kinetic model. The sustained release of drug was observed from a hydrogel-based VDD system, which ensured a steady supply of drug over an extended period and can improve therapeutic outcomes, which can reduce the limitations associated with conventional formulations. Overall, the results of various physico-chemical, drug delivery and biomedical properties of hydrogels suggested that these hydrogels are appropriate materials for vaginal drug delivery applications.

## Ethical statement

This work did not involve the use of human subjects. This work did not involve the use of live animals in laboratory, and no *in vivo* experiments have been performed for this work. The supplier of the goat-intestine membrane and blood was Slaughter House, Lal Pani-Shimla-India and these materials were the waste of Slaughter house. No animal has been directly used in this research.

## Conflicts of interest

There are no conflicts (financial and research) of interest to declare.



## Data availability

All the data supporting this article have been included in the manuscript in the form of tables and figures, and no other research results, software or code is available.

## References

- M. W. Tibbitt, J. E. Dahlman and R. Langer, Emerging frontiers in drug delivery, *J. Am. Chem. Soc.*, 2016, **138**(3), 704–717.
- S. Salave, D. Rana, A. Sharma, K. Bharathi, R. Gupta, S. Khode, D. Benival and N. Kommineni, Polysaccharide Based Implantable Drug Delivery: Development Strategies, Regulatory Requirements, and Future Perspectives, *Polysaccharides*, 2022, **3**, 625–654.
- S. Narala, A. A. Ali Youssef, S. R. Munnangi, N. Narala, P. Lakkala, S. K. Vemula and M. Repka, 3D printing in vaginal drug delivery: a revolution in pharmaceutical manufacturing, *Expet Opin. Drug Deliv.*, 2024, 1–15.
- C. M. Caramella, S. Rossi, F. Ferrari, M. C. Bonferoni and G. Sandri, Mucoadhesive and thermogelling systems for vaginal drug delivery, *Adv. Drug Deliv. Rev.*, 2015, **92**, 39–52.
- H. Kaur, B. Gogoi, I. Sharma, D. K. Das, M. A. Azad, D. D. Pramanik and A. Pramanik, Hydrogels as a Potential Biomaterial for Multimodal Therapeutic Applications, *Mol. Pharm.*, 2024, **21**(10), 4827–4848.
- M. Gosecka and M. Gosecki, Antimicrobial polymer-based hydrogels for the intravaginal therapies—engineering considerations, *Pharmaceutics*, 2021, **13**(9), 1393.
- F. Acarturk, Mucoadhesive vaginal drug delivery systems, *Recent Pat. Drug Deliv. Formul.*, 2009, **3**(3), 193–205.
- C. M. Caramella, S. Rossi, F. Ferrari, M. C. Bonferoni and G. Sandri, Mucoadhesive and thermogelling systems for vaginal drug delivery, *Adv. Drug Deliv. Rev.*, 2015, **92**, 39–52.
- R. R. de Araujo Pereira and M. L. Bruschi, Vaginal mucoadhesive drug delivery systems, *Drug Dev. Ind. Pharm.*, 2012, **38**(6), 643–652.
- S. Rossi, B. Viganì, G. Sandri, M. C. Bonferoni, C. M. Caramella and F. Ferrari, Recent advances in the mucus-interacting approach for vaginal drug delivery: From mucoadhesive to mucus-penetrating nanoparticles, *Expet Opin. Drug Deliv.*, 2019, **16**(8), 777–781.
- C. Valenta, The use of mucoadhesive polymers in vaginal delivery, *Adv. Drug Deliv. Rev.*, 2005, **57**(11), 1692–1712.
- F. Brako, R. Thorogate, S. Mahalingam, B. Raimi-Abraham, D. Q. Craig and M. Edirisinghe, Mucoadhesion of progesterone-loaded drug delivery nanofiber constructs, *ACS Appl. Mater. Interfaces*, 2018, **10**(16), 13381–13389.
- R. Shorey, A. Salaghi, P. Fatehi and T. H. Mekonnen, Valorization of lignin for advanced material applications: a review, *RSC Sustain.*, 2024, **2**(4), 804–831.
- A. S. Hassan, G. M. Soliman, M. F. Ali, M. M. El-Mahdy and G. E. D. A. El-Gindy, Mucoadhesive tablets for the vaginal delivery of progesterone: in vitro evaluation and pharmacokinetics/pharmacodynamics in female rabbits, *Drug Dev. Ind. Pharm.*, 2018, **44**(2), 224–232.
- F. Notario-Pérez, R. Cazorla-Luna, A. Martín-Illana, R. Ruiz-Caro, J. Peña and M. D. Veiga, Tenofvir hot-melt granulation using Gelucire® to develop sustained-release vaginal systems for weekly protection against sexual transmission of HIV, *Pharmaceutics*, 2019, **11**(3), 137.
- N. Hassan, U. Farooq, A. K. Das, K. Sharma, M. A. Mirza, S. Fatima, O. Singh, M. J. Ansari, A. Ali and Z. Iqbal, In Silico Guided Nanoformulation Strategy for Circumvention of Candida albicans Biofilm for Effective Therapy of Candidal Vulvovaginitis, *ACS Omega*, 2023, **8**(7), 6918–6930.
- T. Zhang, H. Lv, Y. Zhang, L. Yu, Y. Li, H. Yan, C. He, D. Zhao, L. Zhao, Y. He and Y. Wang, Long-Lasting Anti-Swelling Sustained-Release Estradiol Hydrogel for Promoting Vaginal Wound Healing, *Adv. Mater.*, 2024, **5**(13), 5644–5657.
- R. Pattanayak, S. Pradhan and S. Mohanty, Utilization of green resource-based Mimosa pudica hydrogel powder in a cellulose acetate-based polymeric membrane as absorbent: a sustainable approach towards female hygiene application, *RSC Sustain.*, 2024, **2**(11), 3525–3545.
- J. Guan, L. Li and S. Mao, Applications of carrageenan in advanced drug delivery, in *Seaweed Polysaccharides*, 2017, pp. 283–303.
- P. J. Caceres, M. J. Carlucci, E. B. Damonte, B. Matsuhira and E. A. Zúñiga, Carrageenans from Chilean samples of *Stenogramme interrupta* (Phylloporaceae): structural analysis and biological activity, *Phytochemistry*, 2000, **53**(1), 81–86.
- M. Luo, B. Shao, W. Nie, X. W. Wei, Y. L. Li, B. L. Wang and Y. Q. Wei, Antitumor and adjuvant activity of  $\lambda$ -carrageenan by stimulating immune response in cancer immunotherapy, *Sci. Rep.*, 2015, **5**(1), 11062.
- G. Ling, T. Zhang, P. Zhang, J. Sun and Z. He, Nanostructured lipid-carrageenan hybrid carriers (NLCCs) for controlled delivery of mitoxantrone hydrochloride to enhance anticancer activity bypassing the BCRP-mediated efflux, *Drug Dev. Ind. Pharm.*, 2016, **42**(8), 1351–1359.
- N. Pettinelli, S. Rodríguez-Llamazares, R. Bouza, L. Barral, S. Feijoo-Bandin and F. Lago, Carrageenan-based physically crosslinked injectable hydrogel for wound healing and tissue repairing applications, *Int. J. Pharm.*, 2020, **589**, 119828.
- L. Li, L. Wang, Y. Shao, Y. E. Tian, C. Li, Y. Li and S. Mao, Elucidation of release characteristics of highly soluble drug trimetazidine hydrochloride from chitosan-carrageenan matrix tablets, *Pharm. Sci.*, 2013, **102**(8), 2644–2654.
- W. G. Dai, L. C. Dong and Y. Q. Song, Nanosizing of a drug/carrageenan complex to increase solubility and dissolution rate, *Int. J. Pharm.*, 2007, **342**(1–2), 201–207.
- F. A. Agili and S. F. Mohamed, Synthesis and Characterization of a Self-Crosslinked Organic Copolymer Kappa-Carrageenan/Polyacrylamide/Cetrimide ( $\kappa$ -CAR/PAAm/CI) Hydrogel with Antimicrobial and Anti-Inflammatory Activities for Wound Healing, *Chemistry*, 2023, **5**(4), 2273–2287.



- 27 M. E. Perotti, A. Pirovano and D. M. Phillips, Carrageenan formulation prevents macrophage trafficking from vagina: implications for microbicide development, *Biol. Reprod.*, 2003, **69**(3), 933–939.
- 28 N. Roy, N. Saha, T. Kitano and P. Saha, Novel hydrogels of PVP–CMC and their swelling effect on viscoelastic properties, *J. Appl. Polym. Sci.*, 2010, **117**(3), 1703–1710.
- 29 K. Nyamayaro, T. Iwase, S. G. Hatzikiriakos and P. Mehrkhodavandi, Cellulose nanocrystal-mediated enhancement of hydrogel anti-swelling and water retention, *RSC Sustain.*, 2024, **2**(5), 1543–1550.
- 30 T. Petkar, M. A. L. Huët, D. Bekah, I. C. Phul, N. Goonoo and A. Bhaw-Luximon, Collagen from skipjack tuna skin waste enhances cellular proliferative activity, vascularization potential and anti-inflammatory properties of nanofibrous and hydrogel scaffolds, *RSC Sustain.*, 2025, **3**(8), 3567–3581.
- 31 Z. Goudarzi and S. Saber-Samandari, Design and Development of a Novel Multiple-Network Hydrogel Composed of Polyacrylamide, Gelatin, and Alginate as a Wound Dressing, *Fibres Polym.*, 2024, **25**(9), 3217–3228.
- 32 P. Farshforoush, S. Ghanbarzadeh, A. M. Goganian and H. Hamishehkar, Novel metronidazole-loaded hydrogel as a gastroretentive drug delivery system, *Iran. J. Polym.*, 2017, **26**, 895–901.
- 33 A. Aka-Any-Grah, K. Bouchemal, A. Koffi, F. Agnely, M. Zhang, M. Djabourov and G. Ponchel, Formulation of mucoadhesive vaginal hydrogels insensitive to dilution with vaginal fluids, *Eur. J. Pharm. Biopharm.*, 2010, **76**(2), 296–303.
- 34 P. L. Ritger and N. A. Peppas, A simple equation for description of solute release I. Fickian and non-fickian release from non-swelling devices in the form of slabs, spheres, cylinders or discs, *J. Contr. Release*, 1987, **5**(1), 23–36.
- 35 P. L. Ritger and N. A. Peppas, A simple equation for description of solute release II. Fickian and anomalous release from swelling devices, *J. Contr. Release*, 1987, **5**(1), 37–42.
- 36 T. K. Kwei and H. M. Zupko, Diffusion in glassy polymers, *J. Polym. Sci., Part B: Polym. Phys.*, 1969, **7**(5), 867–877.
- 37 N. A. Peppas and R. W. Korsmeyer, Dynamically swelling hydrogels in controlled release applications, *Hydrogels Med. Pharm.*, 1987, **3**, 109–136.
- 38 D. Labarre, Improving blood compatibility of polymeric surfaces, *Trends Biomater. Artif. Organs*, 2001, **15**(1), 1–3.
- 39 Y. Imai and Y. Nose, A new method for evaluation of antithrombogenicity of materials, *J. Biomed. Mater. Res.*, 1972, **6**(3), 165–172.
- 40 American Society for Testing and Material, *ASTM F 756-00: Standard Practices for Assessment of Haemolytic Properties of Material*, Philadelphia, 2000.
- 41 M. H. Huang and M. C. Yang, Evaluation of glucan/poly (vinyl alcohol) blend wound dressing using rat models, *Int. J. Pharm.*, 2008, **346**(1), 38–46.
- 42 O. H. Lowry, N. J. Rosebrough, A. L. Farr and R. J. Randall, Protein measurement with the Folin phenol reagent, *J. Biol. Chem.*, 1951, **193**(1), 265–275.
- 43 U. G. Spizzirri, O. I. Parisi, F. Iemma, G. Cirillo, F. Puoci, M. Curcio and N. Picci, Antioxidant–polysaccharide conjugates for food application by eco-friendly grafting procedure, *Carbohydr. Polym.*, 2010, **79**(2), 333–340.
- 44 P. Prieto, M. Pineda and M. Aguilar, Spectrophotometric quantitation of antioxidant capacity through the formation of a phosphomolybdenum complex: specific application to the determination of vitamin E, *Anal. Biochem.*, 1999, **269**(2), 337–341.
- 45 N. Thirawong, J. Nunthanid, S. Puttipipatkachorn and P. Sriamornsak, Mucoadhesive properties of various pectins on gastrointestinal mucosa: an in vitro evaluation using texture analyzer, *Eur. J. Pharm. Biopharm.*, 2007, **67**(1), 132–140.
- 46 A. Emami, S. Shojaei, S. C. da Silva Rosa, M. Aghaei, E. Samiei, A. R. Vosoughi and S. Ghavami, Mechanisms of simvastatin myotoxicity: The role of autophagy flux inhibition, *Eur. J. Pharm. Biopharm.*, 2019, **862**, 172616.
- 47 A. Patil, S. Nangare, P. Mahajan, P. Jain and L. Zawar, Chitosan and neem gum-based polyelectrolyte complex for design of allantoin loaded biocomposite film: In-vitro, ex-vivo, and in-vivo characterization, *Int. J. Biol. Macromol.*, 2024, **263**, 130280.
- 48 O. Yom-Tov, L. Neufeld, D. Seliktar and H. Bianco-Peled, A novel design of injectable porous hydrogels with in situ pore formation, *Actabiomaterialia*, 2014, **10**(10), 4236–4246.
- 49 M. V. Risbud and R. R. Bhonde, Polyacrylamide-chitosan hydrogels: in vitro biocompatibility and sustained antibiotic release studies, *Drug Deliv.*, 2000, **7**(2), 69–75.
- 50 Y. Xin, W. Fei, M. Zhang, Y. Chen, Y. Peng, D. Sun, X. Zheng, X. Zhu, Y. Zhao and C. Zheng, Uterine first-pass effect: Unlocking the potential of vaginally administered ritodrine-loaded thermosensitive gel for uterine drug delivery, *Eur. J. Pharm. Sci.*, 2025, **204**, 106945.
- 51 J. S. Varghese, N. Chellappa and N. N. Fathima, Gelatin–carrageenan hydrogels: Role of pore size distribution on drug delivery process, *Colloids Surf., B*, 2014, **113**, 346–351.
- 52 O. T. Aflorea, I. Nacu, L. Vereștiuc, C. N. Yilmaz, A. D. Panainte, C. A. Peptu, I. G. Ostafe and N. Bibire, In Vitro and Ex Vivo Evaluation of Novel Methacrylated Chitosan-PNIPAAm-Hyaluronic Acid Hydrogels Loaded with Progesterone for Applications in Vaginal Delivery, *Polymers*, 2024, **16**(15), 2160.
- 53 V. E. Santo, A. M. Frias, M. Carida, R. Cancedda, M. E. Gomes, J. F. Mano and R. L. Reis, Carrageenan-based hydrogels for the controlled delivery of PDGF-BB in bone tissue engineering applications, *Biomacromolecules*, 2009, **10**(6), 1392–1401.
- 54 F. Hassanzadeh-Afruzi, M. Forouzandeh-Malati, F. Ganjali, M. M. Salehi, A. Maleki and E. N. Zare, Carrageenan-grafted-poly (acrylamide) magnetic nanocomposite modified with graphene oxide for ciprofloxacin removal from polluted water, *Alex. Eng. J.*, 2023, **82**, 503–517.
- 55 P. Pal, N. Rangra, S. Samanta, A. Aryan, J. P. Pandey and G. Sen, Graft copolymer of PVP—A sutureless, haemostatic bioadhesive for wound healing application, *Polym. Bull.*, 2020, **77**, 5191–5212.



- 56 N. J. Hallab, K. J. Bundy, K. O. Connor, R. L. Moses and J. J. Jacobs, Evaluation of metallic and polymeric biomaterial surface energy and surface roughness characteristics for directed cell adhesion, *Tissue Eng.*, 2001, **7**(1), 55–71.
- 57 G. Sharifzadeh, H. Hezaveh, I. I. Muhamad, S. Hashim and N. Khairuddin, Montmorillonite-based polyacrylamide hydrogel rings for controlled vaginal drug delivery, *Mater. Sci. Eng., C*, 2020, **110**, 110609.
- 58 F. Brako, R. Thorogate, S. Mahalingam, B. Raimi-Abraham, D. Q. Craig and M. Edirisinghe, Mucoadhesion of progesterone-loaded drug delivery nanofiber constructs, *ACS Appl. Mater. Interfaces*, 2018, **10**(16), 13381–13389.
- 59 E. Gomez-Ordenez and P. Ruperez, FTIR-ATR spectroscopy as a tool for polysaccharide identification in edible brown and red seaweeds, *Food Hydrocoll.*, 2011, **25**(6), 1514–1520.
- 60 M. Sahiner, S. Sagbas and B. O. Bitlisli, p(AAm/TA)-based IPN hydrogel films with antimicrobial and antioxidant properties for biomedical applications, *J. Appl. Polym. Sci.*, 2015, **132**(16), 41876.
- 61 M. K. Azeem, A. Islam, M. Rizwan, A. Rasool, N. Gul, R. U. Khan, S. M. Khan and T. Rasheed, Sustainable and environment friendlier carrageenan-based pH-responsive hydrogels: Swelling behavior and controlled release of fertilizers, *Colloid Polym. Sci.*, 2023, **301**(3), 209–219.
- 62 S. Jin, M. Liu, S. Chen and C. Gao, Synthesis, characterization and the rapid response property of the temperature responsive PVP-g-PNIPAM hydrogel, *Eur. Polym. J.*, 2008, **44**(7), 2162–2170.
- 63 K. Eha, T. Pehk, I. Heinmaa, A. Kaleda and K. Laos, Impact of short-term heat treatment on the structure and functional properties of commercial furcellaran compared to commercial carrageenans, *Heliyon*, 2021, **7**(4), e06640.
- 64 R. Meena, K. Prasad, G. Mehta and A. K. Siddhanta, Synthesis of the copolymer hydrogel  $\kappa$ -carrageenan-graft-PAAm: Evaluation of its absorbent and adhesive properties, *J. Appl. Polym. Sci.*, 2006, **102**(6), 5144–5152.
- 65 G. Sen, S. Mishra, K. Prasad Dey and S. Bharti, Synthesis, characterization and application of novel polyacrylamide-grafted barley, *J. Appl. Polym. Sci.*, 2014, **131**(22), 41046.
- 66 N. E. Ben Ammar, R. ESSID, T. Saied, M. Şen, S. Elkahoui and A. H. Hamzaoui, Synthesis and characterization of radiation cross-linked PVP hydrogels and investigation of its potential as an antileishmanial drug carrier, *Polym. Bull.*, 2020, **77**(3), 1343–1357.
- 67 N. A. A. Ghani, R. Othaman, A. Ahmad, F. H. Anuar and N. H. Hassan, Impact of purification on iota carrageenan as solid polymer electrolyte, *Arab. J. Chem.*, 2019, **12**(3), 370–376.
- 68 C. Croitoru, M. A. Pop, T. Bedo, M. Cosnita, I. C. Roata and I. Hulka, Physically crosslinked poly (vinyl alcohol)/kappa-carrageenan hydrogels: structure and applications, *Polymers*, 2020, **12**(3), 560.
- 69 S. Baghel, H. Cathcart and N. J. O'Reilly, Polymeric amorphous solid dispersions: a review of amorphization, crystallization, stabilization, solid-state characterization, and aqueous solubilization of biopharmaceutical classification system class II drugs, *J. Pharm. Sci.*, 2016, **105**(9), 2527–2544.
- 70 P. B. Sutar, R. K. Mishra, K. Pal and A. K. Banthia, Development of pH sensitive polyacrylamide grafted pectin hydrogel for controlled drug delivery system, *J. Mater. Sci.: Mater. Med.*, 2008, **19**, 2247–2253.
- 71 B. Singh and V. Sharma, Designing galacturonic acid /arabinogalactan crosslinked poly(vinylpyrrolidone)- copoly(2-acrylamido-2-methylpropane sulfonic acid) polymers: Synthesis, characterization and drug delivery application, *Polymer*, 2016, **91**, 50–61.
- 72 S. Prabhakar, J. Bajpai and A. K. Bajpai, Fabrication of interpenetrating networks of poly (vinyl alcohol-g-acrylamide) and chitosan-g-polyacrylamide chains and evaluation of water sorption, blood compatibility and cytotoxicity behaviors, *Polym.-Plast. Technol. Mater.*, 2012, **51**(14), 1443–1450.
- 73 F. Sabbagh and I. I. Muhamad, Acrylamide-based hydrogel drug delivery systems: release of acyclovir from MgO nanocomposite hydrogel, *J. Taiwan Inst. Chem. Eng.*, 2017, **72**, 182–193.
- 74 O. T. Afloarea, I. Nacu, L. Vereştiuc, C. N. Yilmaz, A. D. Panainte, C. A. Peptu, I. G. Ostafe and N. Bibire, In Vitro and Ex Vivo Evaluation of Novel Methacrylated Chitosan-PNIPAAm-Hyaluronic Acid Hydrogels Loaded with Progesterone for Applications in Vaginal Delivery, *Polymers*, 2024, **16**(15), 2160.
- 75 X. Huang and C. S. Brazel, On the importance and mechanisms of burst release in matrix-controlled drug delivery systems, *J. Contr. Release*, 2001, **73**(2–3), 121–136.
- 76 H. M. Nizam El-Din, A. W. M. El-Naggar and F. I. Abu-El Fadle, Characterization and drug release kinetics of polyacrylamide/sodium alginate blend hydrogels synthesized by gamma irradiation, *Polym. Bull.*, 2024, **81**(7), 6149–6171.
- 77 N. V. Dubashynskaya, V. A. Petrova, A. V. Sgibnev, V. Y. Elokhovskiy, Y. I. Cherkasova and Y. A. Skorik, Carrageenan/chitin nanowhiskers cryogels for vaginal delivery of metronidazole, *Polymers*, 2023, **15**(10), 2362.
- 78 C. L. Narayana Reddy, B. Y. Swamy, C. V. Prasad, K. Madhusudhan Rao, M. N. Prabhakar, C. Aswini, M. C. S. Subha and K. C. Rao, Development and characterization of chitosan-poly (vinyl pyrrolidone) blend microspheres for controlled release of metformin hydrochloride, *Int. J. Polym. Mater.*, 2012, **61**(6), 424–436.
- 79 M. Cirri, F. Maestrelli, S. Scuota, V. Bazzucchi and P. Mura, Development and microbiological evaluation of chitosan and chitosan-alginate microspheres for vaginal administration of metronidazole, *Int. J. Pharm.*, 2021, **598**, 120375.
- 80 WHO/UNFPA/FHI, *Use and Procurement of Additional Lubricants for Male and Female Condoms: WHO/UNFPA/FHI*, WHO, Geneva, Switzerland, 2012.
- 81 N. Z. Jin and S. C. Gopinath, Potential blood clotting factors and anticoagulants, *Biomed. Pharmacother.*, 2016, **84**, 356–365.



- 82 S. Popov, N. Paderin, D. Khramova, E. Kvashninova, A. Melekhin and F. Vityazev, Characterization and biocompatibility properties in vitro of gel beads based on the pectin and  $\kappa$ -carrageenan, *Mar. Drugs*, 2022, **20**(2), 94.
- 83 S. Tavakoli, M. Kharaziha, S. Nemati and A. Kalateh, Nanocomposite hydrogel based on carrageenan-coated starch/cellulose nanofibers as a hemorrhage control material, *Carbohydr. Polym.*, 2021, **251**, 117013.
- 84 S. Takemoto, Y. Kusudo, K. Tsuru, S. Hayakawa, A. Osaka and S. Takashima, Selective protein adsorption and blood compatibility of hydroxy-carbonate apatites, *J. Biomed. Mater. Res., Part A*, 2004, **69**(3), 544–551.
- 85 P. H. Lima, S. V. Pereira, R. B. Rabello, E. Rodriguez-Castellón, M. M. Beppu, P. Chevallier, D. Mantovani and R. S. Vieira, Blood protein adsorption on sulfonated chitosan and  $\kappa$ -carrageenan films, *Colloids Surf., B*, 2013, **111**, 719–725.
- 86 S. Nie, J. Xue, Y. Lu, Y. Liu, D. Wang, S. Sun, F. Ran and C. Zhao, Improved blood compatibility of polyethersulfone membrane with a hydrophilic and anionic surface, *Colloids Surf., B*, 2012, **100**, 116–125.
- 87 J. Xie and K. M. Schaich, Re-evaluation of the 2, 2-diphenyl-1-picrylhydrazyl free radical (DPPH) assay for antioxidant activity, *J. Agric. Food Chem.*, 2014, **62**(19), 4251–4260.
- 88 L. V. Abad, L. S. Relleve, C. D. T. Racadio, C. T. Aranilla and M. Alumanda, Antioxidant activity potential of gamma irradiated carrageenan, *Appl. Radiat. Isot.*, 2013, **79**, 73–79.
- 89 L. Y. Madruga, R. M. Sabino, E. C. Santos, K. C. Papat, R. D. C. Balaban and M. Kipper, JCarboxymethyl-kappa-carrageenan: A study of biocompatibility, antioxidant and antibacterial activities, *Int. J. Biol. Macromol.*, 2020, **152**, 483–491.
- 90 J. C. Sanchez-Rangel, J. Benavides, J. B. Heredia, L. Cisneros-Zevallos and D. A. Jacobo-Velázquez, The Folin–Ciocalteu assay revisited: improvement of its specificity for total phenolic content determination, *Anal. Methods*, 2013, **5**(21), 5990–5999.
- 91 A. Phonchai, Y. Kim, R. Chantiwas and Y. K. Cho, Lab-on-a-disc for simultaneous determination of total phenolic content and antioxidant activity of beverage samples, *Lab Chip*, 2016, **16**(17), 3268–3275.
- 92 N. Bibi Sadeer, D. Montesano, S. Albrizio, G. Zengin and M. F. Mahomoodally, The versatility of antioxidant assays in food science and safety—Chemistry, applications, strengths, and limitations, *Antioxidants*, 2020, **9**(8), 709.
- 93 L. M. d. M. C. Ferreira, N. F. D. Cruz, D. G. Lynch, P. F. D. Costa, C. G. Salgado, J. O. C. Silva-Júnior and R. M. Ribeiro-Costa, Hydrogel Containing Propolis: Physical Characterization and Evaluation of Biological Activities for Potential Use in the Treatment of Skin Lesions, *Pharmaceuticals*, 2024, **17**(10), 1400.
- 94 J. Tosic-Pajic, D. Seklic, J. Radenkovic, S. Markovic, J. Cukic, D. Baskic, S. Popovic, M. Todorovic and P. Sazanović, Augmented oxidative stress in infertile women with persistent chlamydial infection, *Reprod. Biol.*, 2017, **17**(2), 120–125.
- 95 S. Gupta, V. Kakkar and I. Bhushan, Crosstalk between vaginal microbiome and female health: a review, *Microb. Pathog.*, 2019, **136**, 103696.
- 96 N. Kalia, J. Singh and M. Kaur, Microbiota in vaginal health and pathogenesis of recurrent vulvovaginal infections: a critical review, *Ann. Clin. Microbiol. Antimicrob.*, 2020, **19**, 1–19.
- 97 D. F. Williams, Biocompatibility pathways: biomaterials-induced sterile inflammation, mechanotransduction, and principles of biocompatibility control, *ACS Biomater. Sci. Eng.*, 2017, **3**(1), 2–35.
- 98 S. Losada-Barreiro and C. Bravo-Diaz, Free radicals and polyphenols: The redox chemistry of neurodegenerative diseases, *Eur. J. Med. Chem.*, 2017, **133**, 379–402.
- 99 L. Feng, L. Wang, Y. Ma, W. Duan, S. Martin-Saldaña, Y. Zhu, X. Zhang, B. Zhu, C. Li, S. Hu and M. Bao, Engineering self-healing adhesive hydrogels with antioxidant properties for intrauterine adhesion prevention, *Bioact. Mater.*, 2023, **27**, 82–97.
- 100 J. Liu, X. Han, T. Zhang, K. Tian, Z. Li and F. Luo, Reactive oxygen species (ROS) scavenging biomaterials for anti-inflammatory diseases: From mechanism to therapy, *J. Hematol. Oncol.*, 2023, **16**(1), 116.
- 101 J. D. Smart, I. W. Kellaway and H. E. C. Worthington, An in-vitro investigation of mucosa-adhesive materials for use in controlled drug delivery, *J. Pharm. Pharmacol.*, 1984, **36**(5), 295–299.
- 102 Y. Liu, Y. Y. Zhu, G. Wei and W. Y. Lu, Effect of carrageenan on poloxamer-based in situ gel for vaginal use: Improved in vitro and in vivo sustained-release properties, *Eur. J. Pharm. Sci.*, 2009, **37**(3–4), 306–312.
- 103 E. M. Pacheco-Quito, R. Ruiz-Caro, J. Rubio, A. Tamayo and M. D. Veiga, Carrageenan-based acyclovir mucoadhesive vaginal tablets for prevention of genital herpes, *Mar. Drugs*, 2020, **18**(5), 249.
- 104 S. Mansuri, P. Kesharwani, K. Jain, R. K. Tekade and N. K. Jain, Mucoadhesion: A promising approach in drug delivery system, *React. Funct. Polym.*, 2016, **100**, 151–172.
- 105 M. P. Sánchez-Sánchez, A. Martín-Illana, R. Ruiz-Caro, P. Bermejo, M. J. Abad, R. Carro, L. M. Bedoya, A. Tamayo, J. Rubio, A. Fernández-Ferreiro and F. Otero-Espinar, Chitosan and kappa-carrageenan vaginal acyclovir formulations for prevention of genital herpes. In vitro and ex vivo evaluation, *Mar. Drugs*, 2015, **13**(9), 5976–5992.
- 106 P. Van der Bijl and A. D. van Eyk, Comparative in vitro permeability of human vaginal, small intestinal and colonic mucosa, *Int. J. Pharm.*, 2003, **261**(1–2), 147–152.
- 107 F. Tugcu-Demiroz, S. Saar, S. Tort and F. Acartürk, Electrospun metronidazole-loaded nanofibers for vaginal drug delivery, *Drug Dev. Ind. Pharm.*, 2020, **46**(6), 1015–1025.
- 108 W. Li, J. Zhou and Y. Xu, Study of the in vitro cytotoxicity testing of medical devices, *Biomed. Rep.*, 2015, **3**(5), 617–620.
- 109 R. Yegappan, V. Selvaprithiviraj, S. Amirthalingam, A. Mohandas, N. S. Hwang and R. Jayakumar, Injectable



- angiogenic and osteogenic carrageenan nanocomposite hydrogel for bone tissue engineering, *Int. J. Biol. Macromol.*, 2019, **122**, 320–328.
- 110 S. Ashe, S. Behera, P. Dash, D. Nayak and B. Nayak, Gelatin carrageenan sericin hydrogel composites improves cell viability of cryopreserved SaOS-2 cells, *Int. J. Biol. Macromol.*, 2020, **154**, 606–620.
- 111 S. M. Khade, B. Behera, S. S. Sagiri, V. K. Singh, A. Thirugnanam, K. Pal, S. S. Ray, D. K. Pradhan and M. K. Bhattacharya, Gelatin-PEG based metronidazole-loaded vaginal delivery systems: preparation, characterization and in vitro antimicrobial efficiency, *Iran. Polym. J.*, 2014, **23**, 171–184.
- 112 A. D. Permana, R. M. Asri, M. N. Amir, A. Himawan, A. Arjuna, N. Juniarti and S. A. Mardikasari, Development of thermoresponsive hydrogels with mucoadhesion properties loaded with metronidazole gel-flakes for improved bacterial vaginosis treatment, *Pharmaceutics*, 2023, **15**(5), 1529.
- 113 E. Sulastri, M. S. Zubair, R. Lesmana, A. F. A. Mohammed and N. Wathoni, Development and characterization of ulvan polysaccharides-based hydrogel films for potential wound dressing applications, *Drug Des. Dev. Ther.*, 2021, 4213–4226.
- 114 D. Anokwah, E. A. Kwatia, I. K. Amponsah, Y. Jibira, B. K. Harley, E. O. Ameyaw and A. Y. Mensah, Evaluation of the anti-inflammatory and antioxidant potential of the stem bark extract and some constituents of *Aidiagenipiflora* (DC.) dandy (rubiaceae), *Heliyon*, 2022, **8**(8), e10082.
- 115 A. C. Hearps, D. Tyssen, D. Srbinovski, L. Bayigga, D. J. D. Diaz, M. Aldunate, R. A. Cone, R. Gugasyan, D. J. Anderson and G. Tachedjian, Vaginal lactic acid elicits an anti-inflammatory response from human cervicovaginal epithelial cells and inhibits production of pro-inflammatory mediators associated with HIV acquisition, *Mucosal Immunol.*, 2017, **10**(6), 1480–1490.
- 116 R. Solanki, M. Dhanka, P. Thareja and D. Bhatia, Self-healing, injectable chitosan-based hydrogels: structure, properties and biological applications, *Adv. Mater.*, 2024, **5**(13), 5365–5393.
- 117 A. Martín-Illana, F. Notario-Pérez, R. Cazorla-Luna, R. Ruiz-Caro and M. D. Veiga, Smart freeze-dried bigels for the prevention of the sexual transmission of HIV by accelerating the vaginal release of tenofovir during intercourse, *Pharmaceutics*, 2019, **11**(5), 232.
- 118 T. A. Jackson, Y. P. Neo, S. P. Sisinthy and B. Gorain, Delivery of therapeutics from layer-by-layer electrospun nanofiber matrix for wound healing: An update, *J. Pharm. Sci.*, 2021, **110**(2), 635–653.
- 119 K. R. Park and Y. C. &Nho, Synthesis of PVA/PVP hydrogels having two-layer by radiation and their physical properties, *Radiat. Phys. Chem.*, 2003, **67**(3–4), 361–365.
- 120 M. B. Salehi, A. M. Moghadam and S. Z. Marandi, Polyacrylamide hydrogel application in sand control with compressive strength testing, *Pet. Sci.*, 2019, **16**, 94–104.
- 121 M. Brandt, C. Abels, T. May, K. Lohmann, I. Schmidts-Winkler and U. B. Hoyme, Intravaginally applied metronidazole is as effective as orally applied in the treatment of bacterial vaginosis, but exhibits significantly less side effects, *Eur. J. Obstet. Gynecol. Reprod. Biol.*, 2008, **141**(2), 158–162.
- 122 A. D. Permana, R. M. Asri, M. N. Amir, A. Himawan, A. Arjuna, N. Juniarti and S. A. Mardikasari, Development of thermoresponsive hydrogels with mucoadhesion properties loaded with metronidazole gel-flakes for improved bacterial vaginosis treatment, *Pharmaceutics*, 2023, **15**(5), 1529.
- 123 N. Thakur and B. Singh, Designing biocompatible functional network pH-sensing hydrogels for automated colonic therapeutic delivery, *New J. Chem.*, 2025, **49**(24), 10357–10378.
- 124 S. Shao, S. Gao, Y. Li and Y. Lv, Rapid screening and synthesis of abiotic synthetic receptors for selective bacterial recognition, *ACS Appl. Mater. Interfaces*, 2023, **15**(13), 16408–16419.
- 125 R. Zhang, T. Zhang, Y. Lv, P. Qin, H. Li, J. Li and T. Tan, Selective binding of heparin oligosaccharides in a magnetic thermoresponsive molecularly imprinted polymer, *Talanta*, 2019, **201**, 441–449.

